

Reuse within a cell — interference rejection or multiuser detection?

Claes Tidestav, Mikael Sternad
and Anders Ahlén

MAY 1998



UPPSALA UNIVERSITY
Signals and Systems

Abstract

We investigate the use of an antenna array at the receiver in FDMA/TDMA systems to let several users share one communication channel within a cell. A decision feedback equalizer which simultaneously detects all incoming signals (multiuser detection) is compared to a set of decision feedback equalizers, each detecting one signal and rejecting the remaining as interference. We also introduce the existence of a zero-forcing solution to the equalization problem as an indicator of near-far resistance of different detector structures. Near-far resistance guarantees that good performance will be obtained if the channel is known and the noise level is low.

Simulations show that with an increased number of users in the cell, the incremental performance degradation is small for the multiuser detector.

We have applied the proposed algorithms to experimental measurements from an antenna array testbed, implementing the air interface of DCS-1800. The results from these experiments confirm that reuse within a cell is indeed possible, using either an eight-element array antenna or a two-branch diversity sector antenna.

Multiuser detection will in general provide better performance than interference rejection, especially when the power levels of the users differ substantially. The difference in performance is of crucial importance when the available training sequences are short.

Acknowledgements

The authors are very grateful to Dr Sören Andersson, Dr Ulf Forssén, Mr Henrik Damm and Dr Ari Kangas at Ericsson Radio Systems AB for the opportunity to evaluate the algorithms on real data.

Contents

1	Introduction	1
2	Channel models	4
2.1	A multiple-input-multiple-output baseband channel model	4
2.2	Reducing the MIMO model to a SIMO model with colored noise	6
2.3	Antenna correlation	7
3	The multivariable DFE	10
3.1	Design equations	10
3.1.1	The zero-forcing design	11
3.1.2	The MMSE design	11
3.2	Complexity	13
3.3	Near-far resistance, well-posedness and ZF solutions	14
4	Monte Carlo simulations	17
4.1	Known channel coefficients and noise covariances	18
4.1.1	Equal average SNR for all users and uncorrelated antennas	18
4.1.2	Equal average SNR for all users and correlated antennas	19
4.1.3	Different average SNR for the users and uncorrelated antennas . .	20
4.2	Estimated channel coefficients	22
4.2.1	Estimation using the training sequence only	22
4.2.2	Improving channel estimation using the detected symbols	22
5	Application on measured data	25
5.1	The measurements	25
5.2	Estimation of the average C/N	25
5.3	Results	26
6	Discussion and conclusions	28
References		30
Appendices		33
A	Remarks on the structure and design of the MIMO DFE	33
B	Derivation of the MIMO MMSE DFE	35
C	Proof of Lemma 1	38

Chapter 1

Introduction

The high capacity of a wireless cellular communication system is obtained by the division of a geographical area into cells. Each communication channel is used in a fraction of the cells, and by decreasing the cell size, the capacity of the system can be increased.

Reducing the cell size is however expensive. Instead, multi-element antennas, also known as *antenna arrays*, can be used at the receiver to increase the capacity. Antenna arrays can enhance the desired signal and suppress the interference so that each communication channel can be used more frequently across the network, thereby decreasing the so-called *reuse factor*. When all channels are utilized in every cell, the system is said to have reuse factor one.

To increase the capacity of an FDMA or a TDMA cellular system which has reuse factor one, several users within a cell would have to share each available channel; the system must support *reuse within a cell*.¹ This will cause severe co-channel interference at the receiver. Antenna arrays are then indispensable tools for separating the signals from different users. In this paper, we illustrate, compare and explore two ways of using an antenna array at the receiver to accomplish channel reuse within a cell:

1. Detect the signal from one user at a time while treating the other users as interference. In the following, this approach will be denoted *interference rejection* or *interference cancellation*.
2. Detect the signals from all users simultaneously. This approach will be called *multiuser detection*.

Interference rejection has been thoroughly studied for many different transmission environments using different detectors. In [1], interference rejection using linear receivers is studied, whereas decision feedback equalizers are used for the same purpose by Monsen in [2] and by Balaban and Salz in [3]. Decision feedback equalizers are also the topic of [4], but in an adaptive setting. In [5], Bottomley and Jamal use maximum likelihood sequence estimation with spatial interference whitening to suppress intersymbol and co-channel interference. Interference rejection, i.e. taking the covariance matrix of the interference into account, leads to substantial performance improvements in all these papers.

Multiuser detection within a cell using antenna arrays was first suggested by Winters in [6] and [7]. The emphasis of these papers is on frequency *non-selective* channels and linear detectors. In [8] extensions are made to frequency selective channels. Linear

¹This concept is also known as Spatial Division Multiple Access or SDMA.

and non-linear multiuser detectors have been extensively investigated for application in CDMA systems, see e.g. [9], [10], [11] and [12]. Most multiuser detectors for CDMA systems are block detectors. Such detectors are also becoming increasingly popular in TDMA systems for multiuser detection in conjunction with antenna arrays [13], [14]. However, block detection has limitations for time-varying channels, since the detector parameters in that case may have to be updated on a symbol-by-symbol basis. In general, block detectors are also more complex and memory consuming than their symbol-by-symbol counterparts. For these reasons, we shall in this paper restrict our attention to symbol-by-symbol detectors.

As will become evident in the following chapter, the performance of multiuser detectors is mostly superior to that of interference cancellers. This is due to two reasons:

1. Non-linear multiuser detectors can suppress interference more efficiently than non-linear interference cancellers. (This is in contrast to MSE optimal *linear* detectors, such as those used in [7]. An optimally tuned linear multiuser detector is exactly the same detector as a set of optimally tuned linear interference cancellers.)
2. The channel estimation is improved: When utilizing training sequences from all users instead of treating all except one as noise, the estimates of channel and noise statistics will be based on more data. Therefore, the model quality is in general improved, which leads to more precise tuning of the detector.

In this paper we will use *decision feedback equalizers (DFE:s)* to illustrate the influence of these two factors. Throughout the paper, we will compare two equalizer structures:

1. The DFE presented in [4], which rejects interference.
2. The DFE of [15], which detects multiple signals simultaneously.²

To use the multiuser detector presented here, the channels from each user to each antenna element must be estimated. In a TDMA system, this in turn requires that bursts from all users are roughly synchronized, and that different users send different training sequences which are known at the receiver. These requirements are not hard to fulfill for users within a cell. Therefore, some form of multiuser detection seems to be a feasible tool for attaining channel reuse within a cell. Exploiting multiuser detection to reduce interference from transmitters *outside* the cell is more difficult, since the base stations in adjacent cells must in that case be synchronized.

Although the multiuser detector suggested here can be modified for application in CDMA systems, we will focus on its use for TDMA and FDMA systems.

The paper is organized as follows: In Chapter 2 the general multiple-input-multiple-output (MIMO) model of the cellular communication system is presented. The multiuser detector will be based on this model. A single-input-multiple-output (SIMO) model is also derived, by regarding all but one of the received messages as colored noise. The detector performing interference rejection will be based on that model. In Chapter 3, the design equations for the MIMO DFE with multiple inputs and outputs will be presented. We also introduce the existence of a zero-forcing DFE as an indicator of how well the

²This minimum mean square error DFE was first derived in [16]. It resembles the DFE presented in [17], but is derived under the constraint of *realizability* (finite decision delay and causal filters), and generalized for straightforward application to channels with different number of inputs and outputs.

MMSE detector can be expected to operate in a scenario with signals and interferers of unequal power. In Chapter 4, extensive simulations are conducted to illustrate important aspects of the implementation of a system employing reuse within a cell. The simulations also illustrate the difference in performance between multiuser detection and interference rejection. The algorithms presented are applied to measurements collected at an antenna array testbed in Chapter 5. The testbed complies with the air interface standard of DCS-1800. Finally, in Chapter 6, the results are discussed and conclusions are drawn.

Chapter 2

Channel models

We shall now introduce the channel models upon which we base the derivation of the detectors. These baseband models are assumed to be linear and sampled at the symbol rate. They are also assumed to include the effects of pulse shaping and analog modulation. The symbol rate is equal for all users. Finally, we assume the channel models to be *time-invariant* over the duration of a TDMA burst. The motivation for the last assumption is solely simplicity of presentation.¹

2.1 A multiple-input-multiple-output baseband channel model

We consider a case with M transmitters and N receiver antennas. The signal from transmitter j propagates through the discrete-time baseband channel $H_{ij}(z^{-1})$ to receiver antenna i . The channel $H_{ij}(z^{-1})$ is given by

$$H_{ij}(z^{-1}) = H_{ij}^0 + H_{ij}^1 z^{-1} + \cdots + H_{ij}^{L_{ij}} z^{-L_{ij}} \quad (2.1)$$

where H_{ij}^n are complex-valued constants and where z^{-1} represents the unit delay operator.²

The digital signal received at antenna i at the discrete time instant k is denoted $x_i(k)$ and can be expressed as

$$x_i(k) = \sum_{n=1}^M H_{in}(z^{-1}) s_n(k) + v_i(k), \quad (2.2)$$

where $s_j(k)$ is the symbol transmitted from user j and the term $v_i(k)$ corresponds to noise and out-of-cell co-channel interference. Note that signals from transmitters within the cell are explicitly modeled in (2.2). The signals $s_j(k)$ and the noises $v_i(k)$ are assumed to be mutually uncorrelated, zero mean wide sense stationary stochastic signals. Furthermore, all signals $s_j(k)$ $j = 1, \dots, M$ are assumed to be mutually uncorrelated, and white with zero mean. The situation is depicted in Fig. 2.1.

¹In practice, the channels will be time-varying due to carrier frequency offsets and fading. The channel models, detectors and design equations presented here can easily be generalized to the time-varying case, see Chapter 7 of [18].

²For any signal $y(k)$, $z^{-1}y(k) = y(k - 1)$.

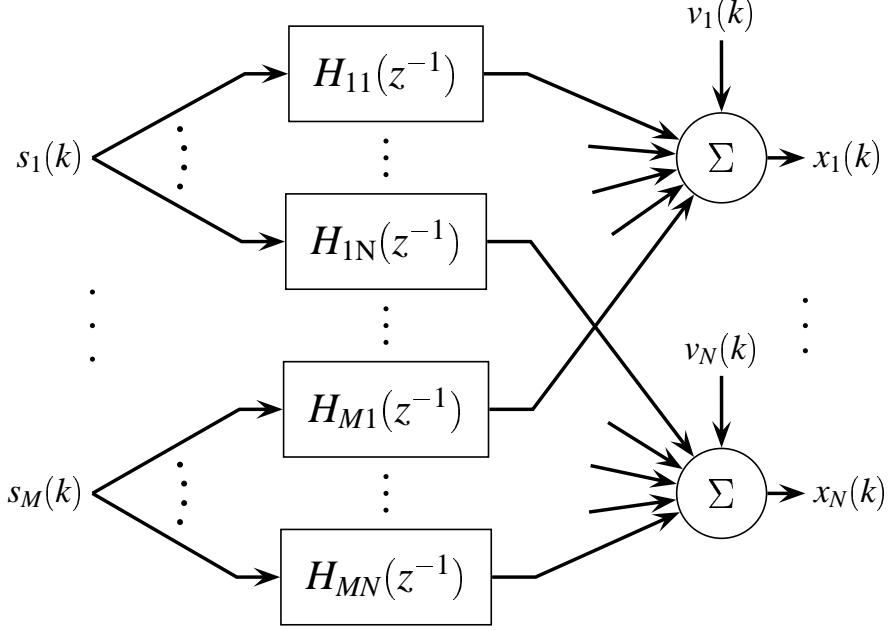


Figure 2.1: The MIMO channel model, where $s_j(k)$ is the symbol transmitted at discrete time instant k from user number j , while $x_i(k)$ is the received sampled baseband signal at antenna i . The signal $v_i(k)$ represents additive noise and out-of-cell co-channel interference.

To obtain a MIMO model, we introduce the signal vectors

$$x(k) = (x_1(k) \quad x_2(k) \quad \dots \quad x_N(k))^T \quad (2.3a)$$

$$s(k) = (s_1(k) \quad s_2(k) \quad \dots \quad s_M(k))^T \quad (2.3b)$$

$$v(k) = (v_1(k) \quad v_2(k) \quad \dots \quad v_N(k))^T. \quad (2.3c)$$

The vector $v(k)$ of noise samples is characterized by the matrix-valued covariance function

$$\psi_{k-m} \triangleq E[v(k)v^H(m)] \quad (2.4)$$

and can be both spatially and temporally colored.³ The vector $x(k)$ of sampled antenna outputs can now be expressed as

$$x(k) = \mathbf{H}(z^{-1})s(k) + v(k) \quad (2.5)$$

$$= \mathbf{H}_0s(k) + \dots + \mathbf{H}_Ls(k-L) + v(k) \quad (2.6)$$

where we have introduced the MIMO impulse response

$$\mathbf{H}(z^{-1}) = \begin{pmatrix} H_{11}(z^{-1}) & \dots & H_{1M}(z^{-1}) \\ \vdots & \ddots & \vdots \\ H_{N1}(z^{-1}) & \dots & H_{NM}(z^{-1}) \end{pmatrix} \quad (2.7)$$

³“Spatial color” refers to the matrix ψ_0 in (2.4) which can be given a spatial interpretation for a particular antenna configuration. When ψ_0 is diagonal, the disturbance is said to be spatially white. Temporal color is, as usual, described by the z-transform of (2.4).

with individual matrix coefficients (taps)

$$\mathbf{H}_p = \begin{pmatrix} H_{11}^p & \dots & H_{1M}^p \\ \vdots & \ddots & \vdots \\ H_{N1}^p & \dots & H_{NM}^p \end{pmatrix}. \quad (2.8)$$

In (2.6),

$$L = \max_{i,j} L_{ij}$$

represents the maximum order of all scalar channels (2.1).

Remark 1. The model (2.6) is rather general, in that it incorporates many different antenna configurations:

1. Phased array systems, where the antenna elements are placed closely together.
2. Diversity systems, where the antennas are usually placed far apart. The large antenna separation helps to reduce the impact of fading.
3. Macro diversity, where multiple base stations communicate simultaneously with a single mobile. This is a special case of a diversity system, described above.

Remark 2. Since the linear model (2.6) is assumed to include the analog modulation, non-linear modulation schemes such as continuous phase modulation (CPM), can in general not be incorporated. Some CPM schemes can, however, with a simple non-linear transformation at the antenna output, be converted to a system which can be modeled as linear with good approximation [19]. Such a system is investigated in Chapter 5.

Remark 3. Although the focus of this paper will be on reuse within a cell, out-of-cell interferers communicating with other base stations could be included among the M users, which are explicitly modeled. The fact that transmission in adjacent cells is in general not synchronized will in that case be a major problem for multiuser detectors.⁴

2.2 Reducing the MIMO model to a SIMO model with colored noise

If we explicitly model the signal from only one of the users, we have to consider signals from the remaining users as interference. Assuming the signal of interest to be signal number 1, we define a disturbance vector $V(k)$ as the sum of all co-channel interference and noise:

$$V(k) = \sum_{n=2}^M \mathbf{H}_n(z^{-1}) s_n(k) + v(k) \quad (2.9)$$

⁴Interference rejection may also suffer from the non-stationary interference resulting from non-synchronized base stations, see [20].

where $\mathbf{H}_n(z^{-1})$ is column n in (2.7). Since all signals $s_j(k)$ are white with unit variance and mutually uncorrelated as well as uncorrelated with the interference $v(k)$, the matrix-valued covariance function of the interference $V(k)$ is given by:

$$\bar{\psi}_{k-m} \triangleq E[V(k)V^H(m)] = \sum_{n=2}^M \sum_{p=\max(0, m-k)}^{\min(L, L-k+m)} \mathbf{H}_n^p (\mathbf{H}_n^{p-k+m})^H + \psi_{k-m} \quad (2.10)$$

where \mathbf{H}_n^p is column n of the impulse response coefficient (2.8) for lag p :

$$\mathbf{H}_n^p = (H_{1n}^p \quad H_{2n}^p \quad \dots \quad H_{Nn}^p)^T. \quad (2.11)$$

The complete single-input-multiple-output channel model thus becomes

$$x(k) = \mathbf{H}_1(z^{-1})s_1(k) + V(k). \quad (2.12)$$

The DFE performing interference rejection will be based on this model.

Remark 4. If the model (2.12) is used as a basis for detector design, estimation of the matrix-valued covariance function of $V(k)$ is vital. This becomes a major problem, since direct estimation of $\bar{\psi}_m$ will provide poor accuracy for the short training sequences typically present in cellular systems. In fact, the estimates of the covariance function will be so unreliable, that we in Section 4.2 and Chapter 5 are forced to exploit only the spatial structure of $V(k)$, i.e. we will assume that $E[V(k)V^H(m)] = 0$ for $k \neq m$.

2.3 Antenna correlation

Spatial diversity has for a long time been used to mitigate fading. The idea is to open multiple uncorrelated channels from the transmitter to the receiver. By combining the signals received through the different channels, the effect of fading can be reduced. If the channels are correlated, the probability of all channels fading simultaneously increases and the advantage of using diversity decreases.

The amount of correlation between the received signals depends on the environment in which the transmitter and receiver antennas are located. When the receiver is surrounded by local scatterers, the received signal will fade. The fading will be uncorrelated at different antenna elements, even when the antenna spacing is rather small. This is the typical situation for the downlink⁵ in a macrocellular system.

When the transmitter but not the receiver is surrounded by local scatterers, the received signal will still fade. However, the fading will *not* be uncorrelated at different antenna elements for small receiver antenna spacings. This is the typical scenario for uplink transmission⁶ in macrocellular environments.

The correlation will depend on the distribution of the scatterers surrounding the transmitter, but different scatterer distributions give similar results [21]. In this paper, we will use an uplink model first suggested in [22], which assumes a uniform linear array at the base station receiver and a large number of scatterers located on a circle around the mobile transmitter. This situation is depicted in Fig. 2.2.

We will treat each scatterer as a secondary transmitter. Assuming that the transmitted signal is narrowband, the signal replicas originating from one such secondary transmitter

⁵Transmission from the base station to the mobile, also known as the forward link.

⁶Transmission from the mobile to the base station, also known as the reverse link.

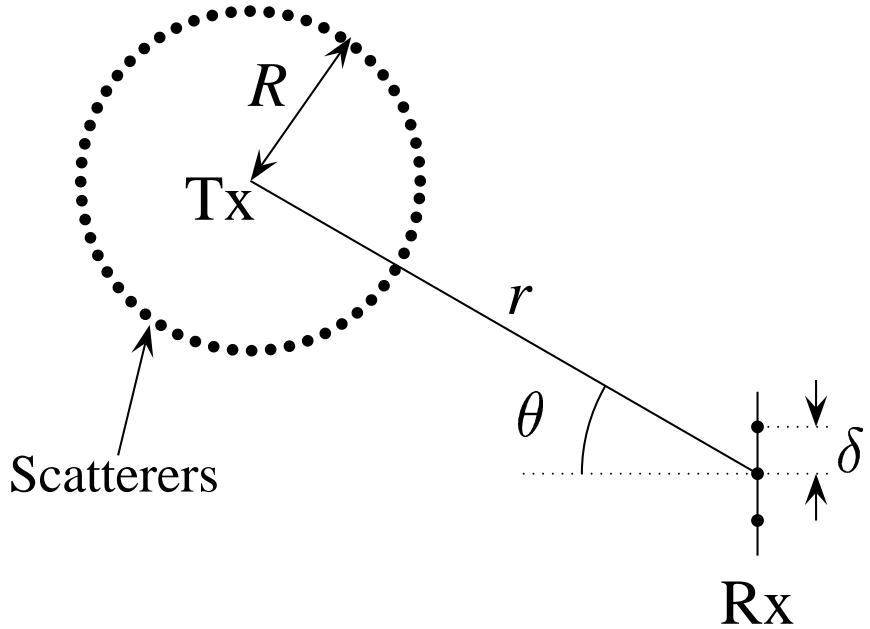


Figure 2.2: Geometry of local scatterers surrounding the transmitter which results in correlation among the antenna elements of a uniform linear array at the receiver.

and received at different antenna elements will be identical except for a phase shift. The complex correlation coefficient between the received baseband signals $x_i(k)$ and $x_{i+1}(k)$ at two antenna elements i and $i + 1$ respectively is denoted as

$$\frac{E[x_i(k)x_{i+1}^*(k)]}{E[|x_i(k)|]E[|x_{i+1}(k)|]} \triangleq \rho(\delta, R, r, \theta). \quad (2.13)$$

We insert the expression (2.2) with $M = 1$ and $v_i(k) = v_{i+1}(k) = 0$ into (2.13). Since the transmitted signal is narrowband, $L_{ij} = L_{(i+1)j} = 0$. By assuming that the channel taps are uncorrelated with the transmitted signal, the expression (2.13) reduces to

$$\rho(\delta, R, r, \theta) = \frac{E[H_{i1}^0(H_{(i+1)1}^0)^*]}{E[|H_{i1}^0|]E[|H_{(i+1)1}^0|]}. \quad (2.14)$$

For the circular scatterer distribution depicted in Fig. 2.2, Fulghum *et al* [23] obtained the following approximation for the antenna correlation:

$$\rho(\delta, R, r, \theta) = J_0\left(\frac{2\pi\delta R}{r}\cos\theta\right)e^{-j2\pi\delta\sin\theta} \quad (2.15)$$

where

δ = the antenna separation, expressed in carrier wavelengths

R = the diameter of the ring of scatterers

r = the distance between the receiver and the transmitter

θ = the angle of the incoming signal with respect to antenna broadside,

and where J_0 is the Bessel function of the first kind and order zero. Equation (2.15) is a good approximation when δ and R are both small relative to r .

In a realistic scenario, the transmitted signal will not be narrowband and $L_{ij} > 0$. In this case, (2.13) will not reduce to (2.14). We will, however, still assume that the

correlation within each column of the $L + 1$ taps can be computed from (2.15), and that each of the $L + 1$ taps is caused by a different ring of scatterers.

The impact of antenna correlation on the performance of the multivariable DFE will be investigated in Section 4.1.2.

Chapter 3

The multivariable DFE

3.1 Design equations

We shall use a multivariable DFE with a transversal feedforward filter and a transversal feedback filter:

$$\begin{aligned}\hat{s}(k - \ell|k) &= \mathbf{S}(z^{-1})x(k) - \mathbf{Q}(z^{-1})\tilde{s}(k - \ell - 1) \\ \tilde{s}(k - \ell) &= f(\hat{s}(k - \ell|k)) .\end{aligned}\quad (3.1)$$

Here, $x(k)$ is the output of the array, used as input to the equalizer and $\tilde{s}(k - \ell - 1)$ are the decisions previously made by the equalizer. The soft estimate $\hat{s}(k - \ell|k)$ is passed through the decision non-linearity $f(\cdot)$ to produce the hard estimate $\tilde{s}(k - \ell)$. The *feedforward filter* $\mathbf{S}(z^{-1})$ is of order n_s with N inputs and M outputs, whereas the *feedback filter* $\mathbf{Q}(z^{-1})$ is of order n_Q and has M inputs and M outputs. A set of M MISO DFE:s can be represented in the same way, the only difference being that the feedback filter $\mathbf{Q}(z^{-1})$ is diagonal. Note that the feedforward filter is causal, and that the decisions on the symbol vectors are made after a finite decision delay ℓ . This means that the DFE is always realizable, in contrast to the DFE:s presented in [3] and [17]. The MIMO DFE is depicted in Fig. 3.1.

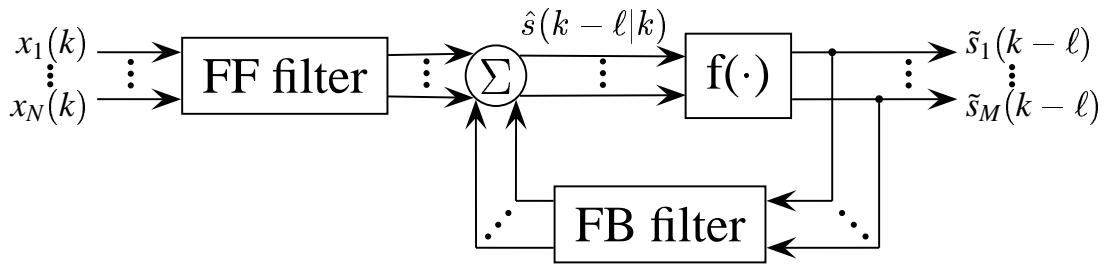


Figure 3.1: The structure of the multivariable DFE, which exploits N sensor signals $x_i(k)$ to compute estimates $\tilde{s}(k - \ell)$ of symbols from M users. The feedforward filter and the feedback filter are both causal and of finite order. A set of MISO DFE:s can be represented in the same way but with a diagonal feedback filter.

The use of FIR filters in (3.1) and the use of model-based (indirect) design of the equalizer is motivated in Appendix A.

To make derivation of optimal equalizer coefficients feasible, we adopt the common assumption that all previous decisions affecting the current symbol estimate are *correct*,

i.e.

$$\tilde{s}(k - \ell - n) = s(k - \ell - n) \quad n = 1, \dots, n_Q + 1. \quad (3.2)$$

Optimal coefficients of the DFE can then be computed from known channel and noise statistics.

Two criteria can be used for the determination of the coefficients of the filters $\mathbf{S}(z^{-1})$ and $\mathbf{Q}(z^{-1})$: The peak distortion criterion and the minimum mean square error (MMSE) criterion.

3.1.1 The zero-forcing design

A scalar equalizer derived by minimizing the peak distortion criterion minimizes the residual intersymbol interference. A scalar equalizer which removes all intersymbol interference is called a *zero-forcing* equalizer. A natural multiuser extension to the peak distortion criterion is to minimize the residual intersymbol *and* co-channel interference [3], and a multiuser zero-forcing (ZF) equalizer can be defined accordingly:

Definition 1: Consider the channel model (2.6) and a multivariable equalizer which forms the estimate $\hat{s}(k - \ell | k)$ of a transmitted symbol vector $s(k - \ell)$. If

$$\hat{s}(k - \ell | k) = s(k - \ell) + \varepsilon(k) \quad (3.3)$$

where $\varepsilon(k)$ is uncorrelated with all transmitted symbol vectors $s(m) \forall m$, then the equalizer is said to be *zero-forcing*.

By substituting (2.5) and (3.2) into (3.1), the zero-forcing condition (3.3) is seen to imply the relation

$$\mathbf{S}(z^{-1})\mathbf{H}(z^{-1})s(k) - \mathbf{Q}(z^{-1})s(k - \ell - 1) = s(k - \ell).$$

A DFE will thus be zero-forcing if and only if $\mathbf{S}(z^{-1})$ and $\mathbf{Q}(z^{-1})$ constitute a solution to the polynomial matrix, or Diophantine, equation [24]

$$\mathbf{S}(z^{-1})\mathbf{H}(z^{-1}) - z^{-\ell-1}\mathbf{Q}(z^{-1}) = z^{-\ell}\mathbf{I}_M. \quad (3.4)$$

3.1.2 The MMSE design

The coefficients of an MMSE equalizer are determined to minimize

$$J = E[||s(k - \ell) - \hat{s}(k - \ell | k)||^2] \quad (3.5)$$

where the expectation is taken over the signal vector $s(k)$ and the noise vector $v(k)$, defined in (2.3b) and (2.3c) respectively.

Under conditions which will be discussed in Section 3.3, the MMSE DFE reduces to the ZF DFE when the covariance matrix of the noise $v(k)$ in (2.6) goes to zero. In the following, we shall focus on the MMSE criterion, since the performance of an MMSE DFE is superior to that of a ZF DFE. A reason for this is that ZF equalizers amplify the additive noise, since the peak distortion criterion is not affected by the noise properties.

The matrix coefficients of the MMSE optimal multivariable decision feedback equalizer can be calculated as follows:

Theorem 1: Consider the multivariable DFE described by (3.1), the channel model (2.6) with M transmitters and N sensors and the noise statistics (2.4), with ψ_0 being non-singular. Assume all M signals $s_j(k)$ to be white with unit variance, to be mutually uncorrelated and uncorrelated with the noise vector $v(k)$. If all past decisions are assumed correct, then the unique matrix polynomials $\mathbf{S}(z^{-1})$ and $\mathbf{Q}(z^{-1})$ in (3.1) of orders n_s and $n_Q = L + n_s - \ell - 1$ respectively, minimizing the MSE (3.5), are obtained as follows:

1. The feedforward filter $\mathbf{S}(z^{-1}) = \mathbf{S}_0 + \mathbf{S}_1 z^{-1} + \cdots + \mathbf{S}_{n_s} z^{-n_s}$ is determined by solving the system of $N(n_s + 1)$ linear equations

$$(\mathcal{F}\mathcal{F}^H + \Psi) \begin{pmatrix} \mathbf{S}_0^H \\ \vdots \\ \mathbf{S}_{n_s}^H \end{pmatrix} = \begin{pmatrix} \mathbf{H}_\ell \\ \vdots \\ \mathbf{H}_0 \\ \mathbf{0} \end{pmatrix} \quad (3.6)$$

with respect to the $N|M$ matrix coefficients \mathbf{S}_n^H , where \mathcal{F} is the $N(n_s+1)|M(\ell+1)$ matrix

$$\mathcal{F} = \begin{pmatrix} \mathbf{H}_0 & \mathbf{H}_1 & \dots & \mathbf{H}_\ell \\ 0 & \mathbf{H}_0 & \dots & \mathbf{H}_{\ell-1} \\ \vdots & \ddots & \ddots & \vdots \\ 0 & \dots & 0 & \mathbf{H}_0 \\ \mathbf{0} & \dots & \dots & \mathbf{0} \end{pmatrix} \quad (3.7)$$

and where

$$\Psi = \begin{pmatrix} \psi_0 & \dots & \psi_{n_s} \\ \vdots & \ddots & \vdots \\ \psi_{-n_s} & \dots & \psi_0 \end{pmatrix}. \quad (3.8)$$

2. The coefficients of the feedback filter $\mathbf{Q}(z^{-1}) = \mathbf{Q}_0 + \mathbf{Q}_1 z^{-1} + \cdots + \mathbf{Q}_{n_Q} z^{-n_Q}$ are given by

$$\mathbf{Q}_n = \sum_{m=\max(0,n-L+\ell+1)}^{\min(n_s,\ell+n+1)} \mathbf{S}_m \mathbf{H}_{\ell+1-m+n} \quad (3.9)$$

where $n_Q = L + n_s - \ell - 1$.

Proof: See Appendix B. ■

Remark 1. The condition that the noise covariance for lag zero, ψ_0 , has full rank ensures that the matrix $\mathcal{F}\mathcal{F}^H + \Psi$ in (3.6) is non-singular. A unique MMSE solution will thus always exist.

Remark 2. To compute a set of MMSE MISO DFE:s, we use Theorem 1 repeatedly for each user of interest, with $M = 1$ and with the noise statistic $\bar{\psi}_n$ described by (2.10) substituted for ψ_n .

Remark 3. Most DFE derivations (see e.g. [3], [17], [25]) assume the presence of a (continuous-time) filter matched to the received signal in front of the DFE. Such matched filtering can be shown to be optimal *only* when the decision delay in the DFE is infinite [26].

Remark 4. For a given detection scenario, the structure of the DFE is determined by the decision delay ℓ , and the degrees of the feedforward filter n_s and the feedback filter n_Q . The impact of these three variables is outlined below.

- The decision delay ℓ is chosen as a trade-off between complexity and performance: the larger decision delay, the better the performance. However, choosing ℓ larger than the delay spread L only leads to minor improvements in performance.
- The degree n_s of the feedforward filter should be chosen as large as possible. However, when the noise is assumed to be temporally white ($\psi_n = 0 \text{ for } n \neq 0$), (3.6) will give $\mathbf{S}_n = 0$ for $n > \ell$.
- The degree n_Q of the feedback filter should be large enough to cancel all postcursor taps (taps with delay $> \ell$) in the linearly equalized channel $\mathbf{S}(z^{-1})\mathbf{H}(z^{-1})$. A lower degree will lead to a loss in performance, and a higher degree will not improve performance. The number of postcursor taps equals $L + n_s - \ell$, so we conclude that $n_Q = L + n_s - \ell - 1$.

3.2 Complexity

To compute the MMSE MIMO or MISO DFE, we need to solve the system of linear equations (3.6) and determine the feedback filter via (3.9). The number of required complex multiplications are indicated in Table 3.1 for both MIMO and MISO DFE:s.

Table 3.1: The number of complex multiplications necessary to compute and run the MIMO DFE and a set of M MISO DFE:s for M users and N sensors. The decision delay of the DFE:s is ℓ , the degree of the feedforward filter is n_s and the delay spread is L . The degree of the feedback filter is $n_Q = L + n_s - \ell - 1$.

	MIMO DFE	MISO DFE
For the feedforward filter $\mathbf{S}(z^{-1})$:		
Calculate $\mathcal{FF}^H + \Psi$	$\frac{1}{4}N^2M(\ell + 1)(\ell + 2)$	
Factorize $\mathcal{FF}^H + \Psi$	$\frac{1}{6}N^3(n_s + 1)^3$	
Solve for the filter coefficients	$N^2(n_s + 1)^2M$	
For the feedback filter $\mathbf{Q}(z^{-1})$:		
Compute the filter coefficients	$M^2N(L + 1)(n_Q + 1)$	$MN(L + 1)(n_Q + 1)$
Equalization of one symbol vector:		
Feedforward filtering	$MN(n_s + 1)$	
Feedback filtering	$M^2N(n_Q + 1)$	$MN(n_Q + 1)$

From Table 3.1, we see that the complexity of a set of MISO DFE:s is clearly comparable to a MIMO DFE for a realistic number of transmitters M . All differences in

complexity arises from the different feedback filters: Both the feedback filter adjustment and the feedback filter operation is more complex for one MIMO DFE than for M MISO DFE:s. However, in a DFE the major complexity resides in the feedforward filter. First, to compute the coefficients of the feedforward filter we need to solve a system of linear equations. Second, the feedforward filter must be implemented with multipliers, whereas the feedback filter typically can be implemented using only adders.

There is however one important case when the MISO DFE is considerably less complex than the MIMO DFE. If only one of the impinging signals is of interest to us, we can use a single MISO DFE to detect that signal. When using a MIMO DFE, we still have to detect all the signals, so the complexity of the MIMO DFE is determined by the total number of impinging signals, not the number of impinging signal of interest. In the uplink, this situation would not be relevant, since the base station must always detect all impinging signals. However, in the downlink the mobile only needs to detect its own signal. In that case, a detector performing interference rejection will be considerably less complex than a multiuser detector.

3.3 Near-far resistance, well-posedness and ZF solutions

An MMSE DFE optimally balances suppression of intersymbol interference and co-channel interference against noise amplification. When the power of the interfering users is large, rejection of these strong signals is of paramount importance, whereas suppression of the noise is less important. In the limit, as the powers of the interfering signals go to infinity, the noise can be neglected.

This situation has been studied extensively for CDMA multiuser detectors, in which case the ability to cope with strong interferers differs among detectors. If a CDMA multiuser detector is able to handle the detection of weak signals (often originating far from the receiver) in the presence of strong (near) interferers, the detector is said to be *near-far resistant* [27].

We may then ask under what conditions are MIMO and MISO DFE:s near-far resistant? To investigate this question, we let the noise covariance ψ_n tend to zero in (2.4) (and (2.10)). If all intersymbol and co-channel interference can be removed, the MMSE equalizer will reduce to a ZF equalizer, and the estimation error will vanish. In this case, perfect equalization is possible, for *any* power of the interfering users. If no ZF equalizer exists, all intersymbol and co-channel interference cannot be removed, so the estimation error will not vanish.

We can therefore use the existence of a ZF DFE as a proof of near-far resistance for the MMSE MIMO DFE or the MMSE MISO DFE. In more general terms, the existence of a zero-forcing solution also indicates that the equalization problem is well-posed in the sense that it can provide a useful solution: good performance can be guaranteed, if the noise level is sufficiently low.

A solution to the zero-forcing equation (3.4) exists if and only if [24]

$$\text{Every common right divisor of } \mathbf{H}(z^{-1}) \text{ and } z^{-\ell-1}\mathbf{I}_M \text{ is also a right divisor of } z^{-\ell}\mathbf{I}_M. \quad (3.10)$$

In general, finding the common divisors of $\mathbf{H}(z^{-1})$ and $z^{-\ell-1}\mathbf{I}_M$ is a non-trivial task. However, when the channel taps $\mathbf{H}_0, \dots, \mathbf{H}_L$ are random matrices with independent elements, $\mathbf{H}(z^{-1})$ and $z^{-\ell-1}\mathbf{I}_M$ have common right divisors with probability zero, in which case a solution to (3.4) exists.

A situation when no zero-forcing solution exists is described in the following lemma:

Lemma 1: Consider equation (3.4). If $M > N$, then $\mathbf{H}(z^{-1})$ and $z^{-\ell-1}\mathbf{I}_M$ have a common right divisor which is not a right divisor of $z^{-\ell}\mathbf{I}_M$, implying that no zero-forcing solution will exist.

Proof: See Appendix C. ■

If (3.10) is fulfilled, we know that a zero-forcing solution exists. However, it remains to specify the filter degrees of such DFE:s. This is the topic of Theorem 2 below. It should be noted that these filter degrees are sufficient but only generically necessary.¹

As a prerequisite, we need the following definitions. We first factorize $\mathbf{H}(z^{-1})$ into three matrix polynomials:

$$\mathbf{H}(z^{-1}) = \bar{\mathbf{H}}(z^{-1})\mathbf{G}(z^{-1})\mathbf{D}(z^{-1}). \quad (3.11)$$

The factors of (3.11) are defined as

$$\mathbf{D}(z^{-1}) \triangleq \text{diag}(z^{-d_1} \dots z^{-d_M}) \quad (3.12a)$$

$$\mathbf{G}(z^{-1}) \triangleq \text{diag}(G_1(z^{-1}) \dots G_M(z^{-1})) \quad (3.12b)$$

$$\bar{\mathbf{H}}(z^{-1}) \triangleq \bar{\mathbf{H}}_0 + \bar{\mathbf{H}}_1 z^{-1} + \dots + \bar{\mathbf{H}}_{\bar{L}} z^{-\bar{L}} \quad (3.12c)$$

where

$$d_j \triangleq \text{the propagation delay for user } j, d_j \leq \ell \quad (3.13a)$$

$$G_j(z^{-1}) \triangleq \begin{aligned} &\text{the greatest common polynomial factor}^2 \text{of the channels} \\ &H_{1j}(z^{-1}), \dots, H_{Nj}(z^{-1}) \text{ from user } j \text{ to all antenna} \\ &\text{elements. Without restriction, } G_j(z^{-1}) \text{ is assumed to be} \\ &\text{monic.} \end{aligned} \quad (3.13b)$$

We also define

$$g_j \triangleq \deg G_j(z^{-1}) \quad (3.14a)$$

$$L_j \triangleq \max_i L_{ij} \quad (3.14b)$$

$$\bar{L}_j \triangleq L_j - d_j - g_j \quad (3.14c)$$

$$\bar{L} \triangleq \max_j \bar{L}_j. \quad (3.14d)$$

We are now ready to formulate Theorem 2.

Theorem 2: Consider the MIMO channel model (2.6) with M sources and N sensors with $M \leq N$ and assume that (3.10) holds. A generically necessary condition for the existence of a zero-forcing MIMO DFE (3.1) with decision delay ℓ and feedforward filter degree n_s is then that

$$n_s \geq \frac{M(\ell+1) - \sum_{m=1}^M d_m}{N} - 1. \quad (3.15)$$

¹Generic necessity of the degree conditions in Theorem 2 should be understood in the sense that when these claims are violated, a zero-forcing equalizer exists with probability zero if the channel taps $\mathbf{H}_0, \dots, \mathbf{H}_L$ are random matrices with independent elements.

²Such a common factor could be caused by e.g. the pulse shaping function.

The condition

$$n_s \geq \max_j \frac{\sum_{m=1}^M \bar{L}_m + \ell + 1 - \bar{L}_j - d_j}{N + 1 - M} - 1 \quad (3.16)$$

is generically necessary for existence of a set of MISO DFE:s with decision delay ℓ and feedforward filter degree n_s .

The condition

$$n_Q \geq L + n_s - \ell - 1 \quad (3.17)$$

is, together with (3.15) and (3.16) respectively, sufficient for the existence of zero-forcing MIMO and MISO DFE:s.

Proof: See Appendix D. ■

Remark 5. If either the condition (3.10) or the degree condition (3.15) or (3.16) is not satisfied, then the corresponding MMSE detector will not work as intended when the signal levels for the interfering users are large. However, the effects of the non-existence of a ZF equalizer will be visible already for moderate signal-to-noise ratios, since the residual co-channel interference will cause bit errors at all noise levels.

Remark 6. The degree limit (3.16) for the MISO DFE will always be higher than the degree condition for the MIMO DFE (3.15).

The impact of a violation of the inequality (3.16) will be demonstrated in Section 4.1.3.

Chapter 4

Monte Carlo simulations

To explore the performance of the MIMO DFE as a tool for joint multiuser detection, extensive simulation experiments are conducted. The experiments are designed to illustrate several key aspects of a real world implementation of a system employing reuse within a cell. We also compare the performance of a multiuser detection approach with the performance of an interference rejection approach.

Some of the simulation scenarios correspond to both uplink and downlink¹ situations. In a few of the scenarios, specific uplink issues are investigated.

In all scenarios, we compare the performance of two MMSE DFE:s:

- One MIMO DFE, performing multiuser detection on all the signals.
- One MISO DFE, detecting one signal while and rejecting the remaining as interference.

Our basic scenario is described next.

- One, two, three and four transmitters ($M = 1, 2, 3, 4$).
- Four receiver antenna elements ($N = 4$).
- Frequency selective, three-tap channels from all transmitters to all receiver antenna elements ($L_{ij} = L = 2$). Each tap is time-invariant during a burst, but subject to Rayleigh fading between bursts. Different taps in a channel fade independently.
- The channels from different transmitters to one receiver antenna are mutually uncorrelated.
- The modulation scheme is BPSK.
- The additive noise is spatially and temporally white ($\psi_m = I_N \delta_m$) and Gaussian distributed with zero mean.
- The smoothing lags and feedforward filter lengths of both DFE:s are chosen equal to the length of the channel impulse response ($\ell = n_s = L = 2$).

In different simulations, the system specified above is investigated under the following additional conditions:

¹For the downlink, we assume that there are several antenna elements at the mobile receiver.

- Known channels (Section 4.1) with
 - Equal average SNR of all users and uncorrelated antennas.
 - Equal average SNR of all users and correlated antennas.
 - Different average SNR of the users and uncorrelated antennas.
- Estimated channels (Section 4.2):
 - Estimation using the training sequence only.
 - Estimation using detected data, with a so-called *bootstrap* method [28].

4.1 Known channel coefficients and noise covariances

In this subsection we shall study the idealized case when all channel coefficients are exactly known. Effects caused by differences in detector structure can here be studied in isolation, since effects of channel estimation errors are avoided.

4.1.1 Equal average SNR for all users and uncorrelated antennas

This is the basic scenario, where all users have the same average SNR, and the channels from a single transmitter to different antenna elements are uncorrelated. In practice, the condition of all users having the same average SNR can be fulfilled by using slow power control, which compensates for the propagation loss and the shadow fading, but not for the Rayleigh fading. The condition of uncorrelated antennas presupposes a sufficiently large antenna spacing δ in Fig. 2.2.

The above scenario is simulated for an average SNR per bit between 0 and 15 dB, where the average SNR per bit [25] for user j , $\bar{\gamma}_b^j$, is defined as

$$\bar{\gamma}_b^j = \frac{1}{N} \frac{E[|H_{ij}^0|^2 + |H_{ij}^1|^2 + |H_{ij}^2|^2] E[|s_j(k)|^2]}{E[|v_i(k)|^2]}, \quad (4.1)$$

where we have divided by N to enable a fair comparison between scenarios with different number of antenna elements.² We assume that $\bar{\gamma}_b^j$ is equal at different antenna elements and thus independent of i .

Fig. 4.1 shows the estimated BER as a function of the average SNR per bit. With four users, the performance of the MIMO DFE at $\bar{\gamma}_b^j = 15$ dB is around 6 dB better than the performance of the MISO DFE. This difference arises from the fact that the MISO DFE uses up all its degrees of freedom to cancel the interference from the other users. This task is easier for the MIMO DFE since its feedback filter takes care of some of the suppression of the co-channel interferers. For fewer users, the difference between the two approaches is smaller. For example, in the case of three users the gain is approximately 3 dB and for two users around 1 dB.

For $\bar{\gamma}_b^j = 15$ dB, the performance degradation when using a MIMO DFE is approximately 1 dB for two users, 3 dB for three users and 5 dB for four users as compared to a single user system. See Table 4.1 for a performance summary.

²Thus, we do *not* use the SNR per channel, defined as $\bar{\gamma}_c^j \triangleq N \bar{\gamma}_b^j$. Also note that signals from other users do *not* affect $\bar{\gamma}_b^j$. Adding users will instead increase the resulting BER for a fixed $\bar{\gamma}_b^j$ and thereby demonstrate the performance degradation as a function of the system load.

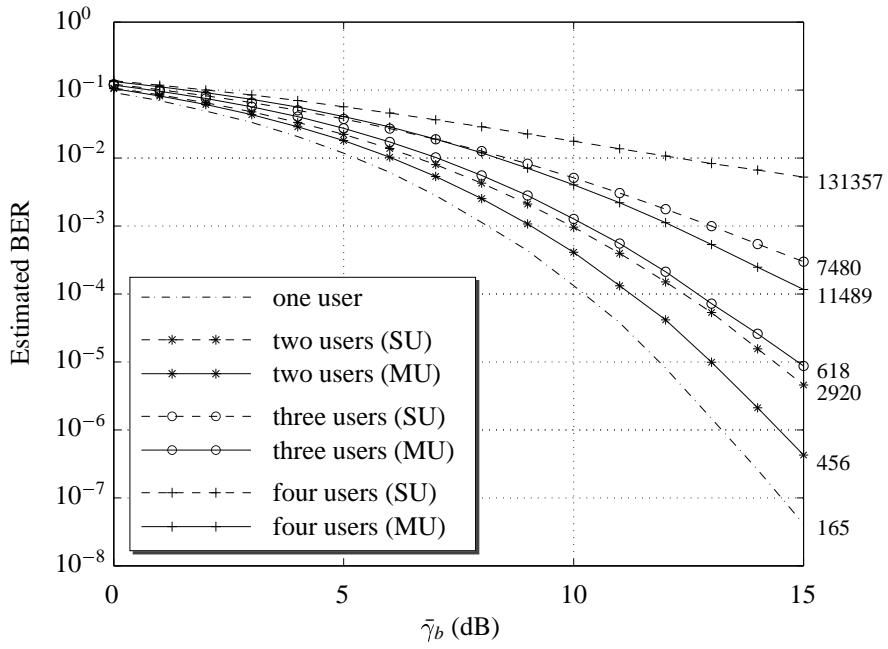


Figure 4.1: Comparison of the MIMO DFE (MU) and the MISO DFE (SU) for known channels, equal transmitter powers and uncorrelated antennas. The numbers to the right of the graph are the number of errors used to estimate the BER for the average SNR per bit $\bar{\gamma}_b=15$ dB.

4.1.2 Equal average SNR for all users and correlated antennas

In a realistic uplink scenario with phased array receivers, the channels from a single user to the different antenna elements will be correlated. This makes the system more susceptible to fading.

However, successful multiuser detection does not require uncorrelated antennas. With perfectly correlated antennas, the antenna array can form narrow beams, which enhance the desired signal and suppress interference, arriving from other directions.

In this simulation, we will assume a uniform linear array with the antenna correlation given by (2.15). In the multipath model, each incoming ray from user j will give rise to a column vector \mathbf{H}_n^p at lag p in the impulse response as defined in (2.11). Each of these column vectors originates from a circular distribution of scatterers as depicted in Fig. 2.2. The angular locations θ of scatterer distributions corresponding to different column vector taps in the impulse response are assumed to be independent stochastic variables, uniformly distributed in the interval $[-90^\circ, 90^\circ]$. The antenna correlations according to (2.15) will depend on the angles θ , which are not under the system designer's control. Therefore, we shall address the performance of the DFE as a function of the correlation coefficient according to (2.15) that would result if the signals would all impinge from an angle $\theta = 0^\circ$, cf. Fig. 2.2:

$$\rho(\delta, R, r, \theta = 0) = J_0\left(\frac{2\pi\delta R}{r}\right) \triangleq \tilde{\rho}\left(\frac{\delta R}{r}\right). \quad (4.2)$$

The quantity $\tilde{\rho}$ can be measured for a given environment and uniform linear array, and the corresponding performance can be predicted from the simulation results presented below.

To calculate the actual antenna correlation ρ for a given value $\tilde{\rho}_0$ of $\tilde{\rho}$, we insert the ratio $R\delta/r$ corresponding to $\tilde{\rho}_0$ and a realization of the stochastic variable θ into (2.15).

The resulting value of ρ is used to form the covariance matrix of \mathbf{H}_n^p . A realization of \mathbf{H}_n^p is then generated. This procedure is repeated for each of $M(L + 1)$ vector taps in the impulse response. The simulation results are presented in Fig. 4.2 for a signal-to-noise ratio of 10 dB and antenna correlations between zero and one.³

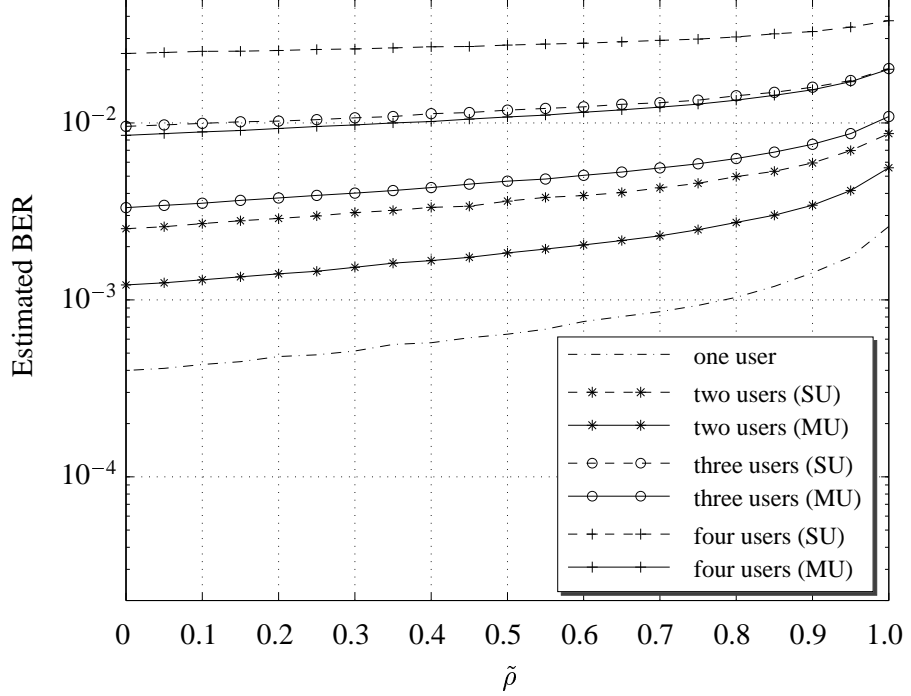


Figure 4.2: Comparison of the MIMO DFE (MU) and the MISO DFE (SU) for a uniform linear array with *correlated antenna elements*. The channels are known and the SNR per bit is $\bar{\gamma}_b = 10$ dB for all users. The estimated BER is shown as a function of the antenna correlation $\tilde{\rho}$ that would result if all signals were impinging at an angle of $\theta = 0^\circ$.

It is evident from Fig. 4.2 that successful multiuser detection and interference rejection are indeed not dependent on uncorrelated antennas. The performance of all algorithms deteriorates when the antenna correlation is increased from zero to one. This is due to the diminished diversity effect, resulting from a decrease in the number of diversity branches from twelve (four uncorrelated antennas and three taps) to three (four perfectly correlated antennas and three taps) per user. However, the multiuser detection approach retains its superior performance as compared to the interference rejection approach.

Remark 1. Notice that $\tilde{\rho} = 0$ does *not* imply that all channel taps are uncorrelated, only that a signal that impinges from $\theta = 0^\circ$ would result in uncorrelated taps. Therefore, the BER for $\tilde{\rho} = 0$ does not coincide with the BER for $\bar{\gamma}_b = 10$ dB in Fig. 4.1, where *all* taps are uncorrelated.

4.1.3 Different average SNR for the users and uncorrelated antennas

In Sections 4.1.1 and 4.1.2, we assumed that power control was used to compensate for the propagation loss and the shadow fading. In the scenario investigated in this subsection,

³While the model (2.15) is not accurate when δ is large relative to r , it still provides a rough estimate of the correlation, which is all that is important here.

we will relax this assumption: Even the average received powers will differ among the users. This will generate the so-called *near-far problem*.

We estimated the BER of a user having an average SNR per bit of 10 dB in a scenario where there are one, two or three additional users, each having an average SNR per bit that is between 0 dB and 10 dB *higher*, i.e. between 10 dB and 20 dB. The result from this simulation is depicted in the *right half* of Fig. 4.3.

In a MIMO DFE, decisions concerning one user affect future symbol estimates of all users. Incorrect decisions on the symbols from a weak user will thus impair the decisions of other, stronger users. In this case, a MISO DFE may yield better performance since (possibly incorrect) decisions of the weaker users' symbols do not influence the estimates the stronger users' symbols.

To investigate this effect, we estimate the BER of a user having an average SNR per bit of 10 dB in a scenario where there were one, two or three additional users, each having an average SNR per bit which was between 0 dB and 10 dB *lower*, i.e. the SNR per bit of the remaining users varied between 10 dB and 0 dB. The result from this simulation is depicted in the *left half* of Fig. 4.3.

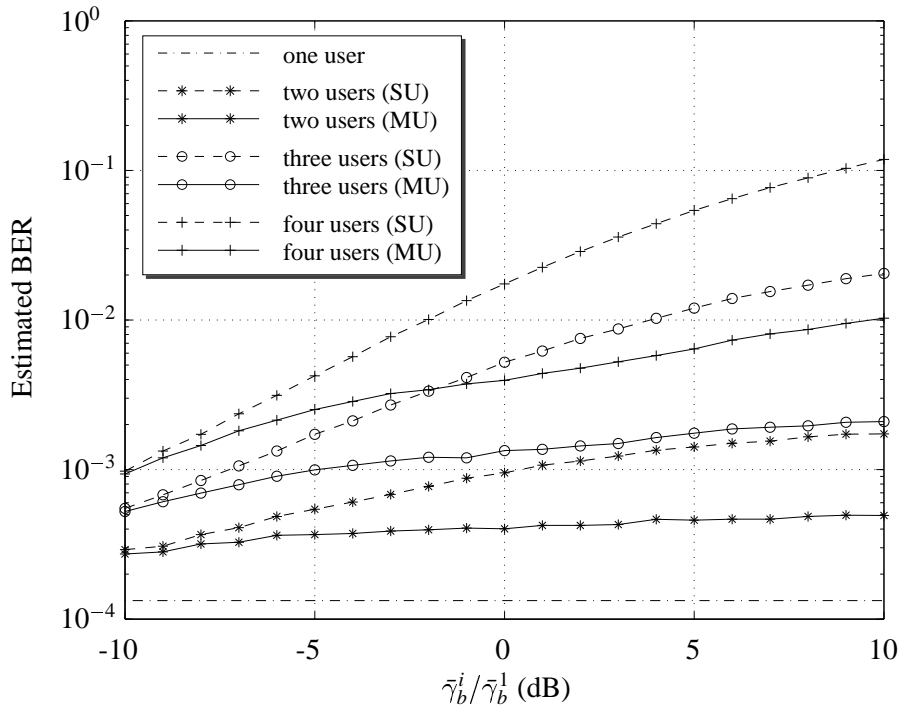


Figure 4.3: Comparison of the MIMO DFE (MU) and the MISO DFE (SU) for known channels, *different transmitter powers* and uncorrelated antennas. In this simulation, 25000 channels were randomly selected. Over each channel, 1000 symbols were transmitted. User number 1 has an SNR per bit of $\bar{\gamma}_b^1 = 10$ dB, while the SNR per bit $\bar{\gamma}_b^i$ of the other users are equal and varies.

From the leftmost part of Fig. 4.3, it is clear that for the investigated differences in power levels, error propagation is not so severe that the BER of a MIMO DFE exceeds the BER of a MISO DFE. On the other hand, from the rightmost part of Fig. 4.3, it is evident that for the MIMO DFE, four users can co-exist in the cell, even when the received average powers differ substantially. For two users, the BER is hardly affected at all by the power level of the interfering user. However, the performance of the MISO DFE is seriously affected by the increase of the power levels of the interfering users, since

this MISO DFE does not comply with the ZF condition (3.16). Inserting numerical values into (3.16) gives the required feedforward filter degree:

$$\begin{aligned} M = 1 &\implies n_s \geq -1/4 \\ M = 2 &\implies n_s \geq 2/3 \\ M = 3 &\implies n_s \geq 2.5 \\ M = 4 &\implies n_s \geq 8 \end{aligned}$$

This means that since we used $n_s = \ell = L = 2$, complete suppression of all co-channel interferers is impossible whenever $M \geq 3$. As the powers of these users increase, the estimation error due to residual interference increases, resulting in an increased BER. The MIMO DFE on the other hand is capable of completely removing the interference from the stronger users, at the expense of a slightly increased noise amplification.

4.2 Estimated channel coefficients

4.2.1 Estimation using the training sequence only

To demonstrate how the MIMO DFE works in a more realistic case, channel estimation is introduced. The data is transmitted in bursts, with a structure similar to that of GSM: A training sequence of 26 symbols is located in the middle of each burst. Together with data symbols, tail symbols and control symbols, this results in a total burst length of 148 symbols.⁴ The channel estimation is performed using the off-line least squares method, and the spatial color of the noise is estimated from the residuals of the channel identification. The temporal color of the noise is not estimated due to the limited amount of data. In the MIMO case, the channels from all users to each antenna element are estimated simultaneously. Apart from this, the simulation conditions are the same as in Section 4.1.1. The results are indicated in Fig. 4.4.

When we compare Figs. 4.1 and 4.4, we see that the difference between the MIMO DFE and the MISO DFE is greater when the channels have to be estimated. The difference between the multiuser detection approach and the interference rejection approach has now increased to about 4 dB for two users, and to about 7 dB for three users and even more for four users. In this case, the overall penalty for squeezing in four users into one cell is about 7 dB as compared to the single user case. Table 4.1 summarizes the performance loss of the MISO DFE and the MIMO DFE for known and estimated channels as compared to the single-user case.

4.2.2 Improving channel estimation using the detected symbols

Since channel estimation errors are a major cause of bit errors in a digital cellular system, there is a great potential for performance improvement in the reduction of the channel estimation errors. One way of accomplishing this would be to use detected symbols as regressors in the estimation algorithm. This approach would thus consist of two passes as follows:

Pass 1:

1. Estimate the channel using the training sequence.

⁴The pulse shaping used in GSM results in a channel with five highly correlated taps. We have not included this feature in the simulation: Only the burst structure resembles the one used in GSM.

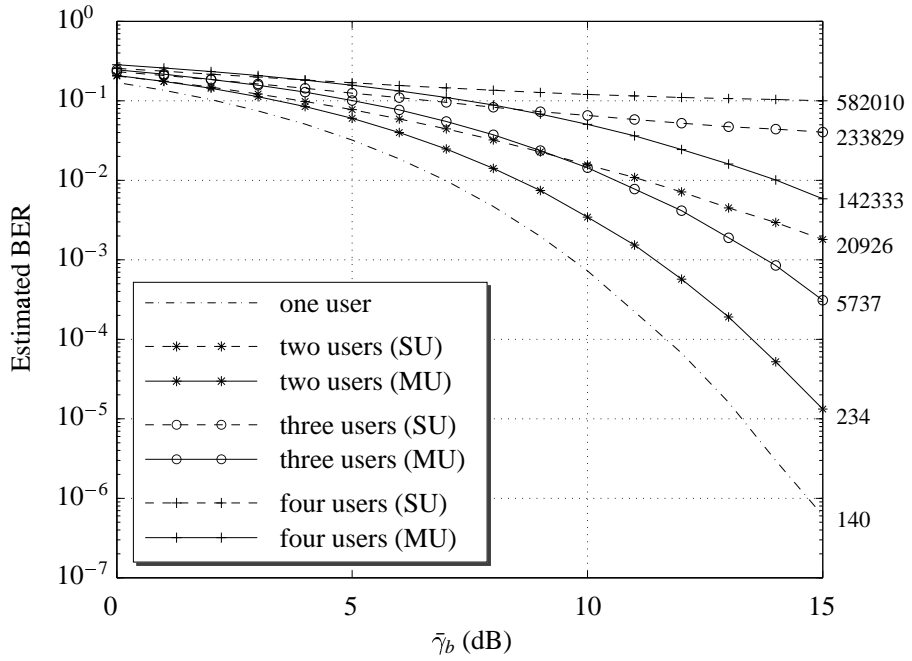


Figure 4.4: Comparison of the MIMO DFE (MU) and the MISO DFE (SU) for estimated channels, equal transmitter powers and uncorrelated antennas. The channel was estimated using *only the training sequence*. The numbers at the right edge of the graph are the number of errors used to estimate the BER for an SNR per bit of $\bar{\gamma}_b=15$ dB.

2. Design an equalizer using these channel estimates.
3. Detect all the symbols in the burst.

Pass 2:

4. Estimate the channel using the training sequence *and* the symbols detected in pass 1.
5. Redesign the equalizer using the updated channel estimates.
6. Repeat the symbol detection.

We thus improve the channel estimates by using detected data which are probably correct. By using these extra regressors we can increase the length of the training sequence from 26 to 148 symbols in the GSM case. This *bootstrap* method is based on the assumption that when the fraction of incorrect decisions from pass 1 is sufficiently small, the channel estimation in pass 2 will provide better accuracy than the channel estimation in pass 1. Bootstrap equalization is discussed in [28] for both decision feedback equalizers and maximum likelihood sequence estimation.

To test this algorithm, we repeat the simulation in Section 4.2.1, with the use of the detected symbols to improve the channel estimates, according to the bootstrap algorithm described above. The results from the second pass of the algorithm are shown in Fig. 4.5.

As can be seen from Fig. 4.5, the BER was reduced when the tentative decisions were used to improve the channel estimates. It seems that the performance of the multiuser detector was impaired more by the poor quality of the channel estimates than the performance of the detector performing interference rejection: The difference between the two approaches is larger when the two pass algorithm is used than when only the training sequence is used to estimate the channel. This is due to the fact that the estimation of the

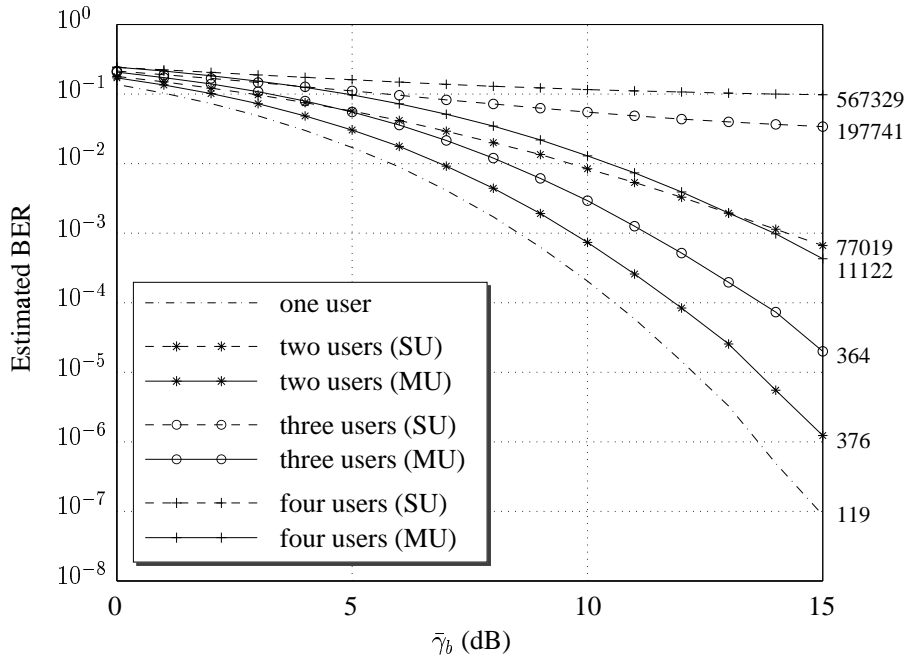


Figure 4.5: Comparison of the MIMO DFE (MU) and the MISO DFE (SU) for estimated channels, equal transmitter powers and uncorrelated antennas. The channel estimates were obtained using *both the training sequence and detected symbols*. The numbers at the right edge of the graph are the number of errors used to estimate the BER for an SNR per bit of $\bar{\gamma}_b=15$ dB.

covariance function of the noise and the interferers is still inaccurate, despite the fact that we now have access to a training sequence of 148 symbols.

The performance at 15 dB of the bootstrap algorithm is summarized in Table 4.1.

Table 4.1: The performance loss experienced when adding users as compared to a single user system for the simulation scenarios in Sections 4.1.1, 4.2.1 and 4.2.2. All values are estimated at an SNR of 15 dB.

Number of users	MISO			MIMO		
	2	3	4	2	3	4
Known channels	2.6 dB	5.6 dB	8.9 dB	1.2 dB	3.0 dB	5.0 dB
Estimated channels using the training sequence only	6.0 dB	10.5 dB	12.9 dB	1.8 dB	4.2 dB	7.3 dB
the two pass algorithm	5.9 dB	11.2 dB	14.0 dB	1.5 dB	3.3 dB	5.6 dB

Chapter 5

Application on measured data

The simulations in Chapter 4 indicate that reuse within a cell is indeed possible. But will it work in practice? To investigate this we will apply the methods described in Chapter 3 to a set of uplink measurements.

5.1 The measurements

The measurements were performed on a testbed constructed by Ericsson Radio Systems AB and Ericsson Microwave Systems AB [29]. The testbed implements the air interface of a DCS-1800 base station. During all measurements, the carrier frequency was 1782 MHz.

The array consists of four antenna elements, each having two polarization diversity branches, resulting in eight antenna outputs. A conventional sector antenna with two branch polarization diversity is also included in the measurement setup for two reasons: To evaluate the impact of using more antenna elements and to estimate the transmitted signal power.

The measurements were performed in Kista, a suburb of Stockholm, Sweden.

A single mobile mounted in a van was used for all experiments. The van drove at approximately 30–40 km/h during the measurement period. The mobile transmitted a burst of data in one of the eight time slots in a GSM frame. The base station down-converted and sampled the received signal and the resulting digital baseband signal was recorded for a large number of frames. This procedure was repeated when the mobile traveled the same route but transmitted another data sequence. The two sets of collected digital baseband measurements were added to represent a situation when two mobile users share the same channel. The algorithms investigated in Chapter 4 were then applied, both to the data recorded at the array antenna, and to the data recorded at the sector antenna.

5.2 Estimation of the average C/N

We estimate the average *carrier-to-noise ratio* (C/N) indirectly, by measuring the received power at the sector antenna when the mobile is inactive. This provides us with an estimate of the noise level. The received power at the sector antenna during the periods when the mobile is active provides an estimate of the signal-plus-noise power. These power level measurements are averaged over a segment of frames. Due to the shadow fading,

this average differs between segments. Thus the performance of the algorithms can be addressed as a function of the average carrier-to-noise ratio.¹

5.3 Results

The frame structure in DCS-1800 is identical to the one described in Section 4.2. In this case, five tap channels are estimated, and $n_s = \ell = L = 4$ is used.

The MMSE MIMO DFE and two MMSE MISO DFE:s were used to demodulate the signals from the two users. In both cases, the bootstrap algorithm described in Chapter 4.2.2 was utilized. The results are shown in Fig. 5.1 for the array antenna and in Fig. 5.2 for the sector antenna.

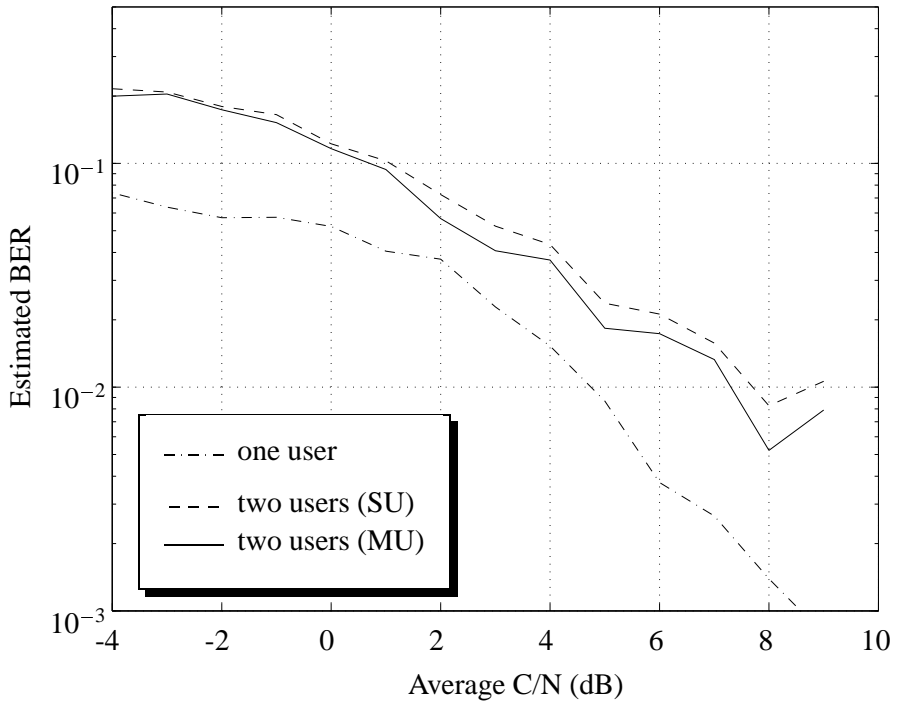


Figure 5.1: Comparison of the MIMO DFE (MU) and the MISO DFE (SU) applied to measurements from a DCS-1800 testbed in a flat fading environment. The antenna array had eight outputs and two users were transmitting simultaneously.

When we compare the results in Fig. 5.1 and 5.2 with the results from the simulations, we see that the error rate decreases much more slowly with SNR for the experimental data than for the simulations. This is because the number of diversity branches is considerably lower in this case: The channel is in fact flat fading and the partial response GMSK modulation causes all the intersymbol interference.

The results from the experiments on the measurements from the array antenna are not surprising. For the lightly loaded system with $N = 8$ and $M = 2$, the performance of a MIMO DFE should be only slightly better than the performance of two MISO DFE:s.

For the sector antenna, the results are more surprising: A MIMO DFE:s performs slightly *worse* than two MISO DFE:s. The reasons for this are twofold:

¹The carrier-to-noise ratio corresponds to the SNR per channel discussed previously. We use the notation C/N rather than SNR to stress the fact that the quantity has been estimated indirectly.

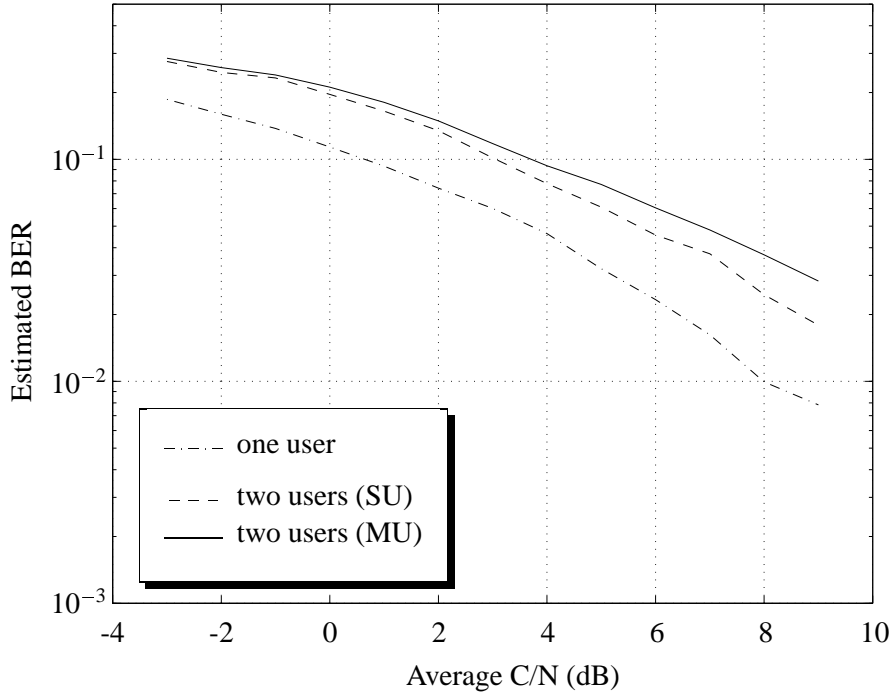


Figure 5.2: Comparison of the MIMO DFE (MU) and the MISO DFE (SU) applied to measurements from a DCS-1800 testbed in a flat fading environment. The sector antenna had two outputs and two users were transmitting simultaneously.

1. Since the channel is flat fading, the MISO DFE will have adequate degrees of freedom. The intersymbol interference induced by the GMSK modulation will be present in the channels to all antenna elements. Hence, each column of $\mathbf{H}(z^{-1})$ will have a common factor of degree L . For $N = 2$ and $M = 2$, the zero-forcing condition (3.16) then reduces to

$$n_s \geq \frac{\sum_{m=1}^2 0 + \ell + 1 - 0 - d_j}{2 + 1 - 2} - 1 = \ell - d_j$$

where ℓ is the decision delay and d_j is the propagation delay of user j . Therefore, the choice $n_s = \ell$ ensures the existence of a ZF MISO DFE for this scenario, and the corresponding MMSE detector will work well.

2. When the amount of intersymbol interference caused by multipath propagation is small, spatial-only interference rejection is sufficient to suppress the interfering user. The MIMO DFE tries to reject co-channel interference by means of an estimate of its spatio-temporal color. This will here lead to *worse* performance, since parameters, which do not improve equalization, are estimated.

It should be noted, that the investigated scenario constitutes a very difficult detection problem: The two mobiles travel exactly the same measurement route. Still, reuse within a cell is possible, using either the array antenna or the sector antenna: The detector performance is approximately 2 dB worse for two users than for one user.

Chapter 6

Discussion and conclusions

In our investigation of receiver algorithms designed to accomplish channel reuse within cells, we have compared MIMO DFE:s which work as multiuser detectors to the use of interference rejection, implemented by MISO DFE:s. Realizable MMSE equalizers of both kinds have been derived, based on channel models and noise spectral models.

In summary, extensive simulations indicate that channel reuse within a cell is indeed a viable option, with multiuser detection providing superior performance. Up to four users could co-exist in the same cell if the receivers utilize antenna arrays with only four antenna elements. With multiuser detection, the price paid for this in increased bit error rate is rather small. We have tested the algorithms on experimental measurements from a DCS-1800 testbed. For the investigated scenario, reuse within a cell is possible using either an eight-element antenna array or a two-branch diversity sector antenna.

Differences in performance between multiuser detection and interference rejection are partly due to the detector *structures*: A multiuser (MIMO) DFE utilizes feedback from previously estimated symbols from *all* users, while the interference rejecting (MISO) DFE performs decision feedback from the user of interest only.

The difference also results from the preconditions for *channel estimation*: In the multiuser case, input-output transfer functions from each user to each antenna can, and must, be estimated. For interference rejection, the co-channel interference constitutes colored noise. The multivariate noise models estimated from short data records will have poor accuracy.

These factors will in general result in a higher performance for the multiuser detector. This is particularly apparent when the detectors are applied to heavily loaded systems (with many users/interferers) and when the delay spread in the multipath channel is large. When applied to lightly loaded systems or when the channels are flat fading, the difference will be small if the estimates of channels and noise statistics have adequate precision. When noise models are inaccurate, the performance difference will still be significant.

Both multiuser detectors and interference rejecting MISO DFE:s can be made near-far resistant. However, the conditions for this, as indicated by the existence of a zero-forcing solution, are more restrictive when using interference rejection.

As topics for further research, multiuser detectors could be useful also for the rejection of out-of-cell co-channel interference. This would require the transmission of training sequences to be synchronized throughout the cellular system.

Our conclusions are based on studies and comparisons of symbol-by-symbol decision feedback equalizers. We would expect similar conclusions to hold from a comparison of joint multiuser maximum likelihood detectors [30] to single-user maximum likelihood

detectors with spatial interference whitening [5]. However, for maximum likelihood detectors the complexity of the two approaches would differ substantially, in contrast to the complexity of the two detectors described here.

Bibliography

- [1] Martin V. Clark, Larry J. Greenstein, William K. Kennedy, and Mansoor Shafi, “Optimum linear diversity receivers for mobile communications,” *IEEE Transactions on Vehicular Technology*, vol. 43, no. 1, pp. 47–56, Feb. 1994.
- [2] Peter Monsen, “MMSE equalization of interference on fading diversity channels,” *IEEE Transactions on Communications*, vol. 32, no. 1, pp. 5–12, Jan. 1984.
- [3] Philip Balaban and Jack Salz, “Optimum diversity combining and equalization in digital data transmission with applications to cellular mobile radio — part I: Theoretical considerations,” *IEEE Transactions on Communications*, vol. 40, no. 5, pp. 885–894, 1992.
- [4] Norm K. Lo, David D. Falconer, and Asrar U.H. Sheikh, “Adaptive equalization for a multipath fading environment with interference and noise,” in *Proceedings of the IEEE Vehicular Technology Conference*, Stockholm, Sweden, June 1994, vol. 1, pp. 252–256.
- [5] Gregory E. Bottomley and Karim Jamal, “Adaptive arrays and MLSE equalization,” in *Proceedings of the IEEE Vehicular Technology Conference*, Chicago, July 1995, vol. 1, pp. 50–54.
- [6] Jack Winters, “On the capacity of radio communication systems with diversity in a Rayleigh fading environment,” *IEEE Journal on Selected Areas in Communications*, vol. 5, no. 5, pp. 871–878, June 1987.
- [7] Jack Winters, “Optimum combining for indoor radio systems with multiple users,” *IEEE Transactions on Communications*, vol. 35, no. 11, pp. 1222–1230, Nov. 1987.
- [8] Jack Salz and Jack Winters, “Effect of fading correlation on adaptive arrays in digital wireless communication,” in *Proceedings of the IEEE Vehicular Technology Conference*, St. Louis, May 1993, pp. 1768–1774.
- [9] Sergio Verdú, “Minimum probability of error for asynchronous gaussian multiple access channels,” *IEEE Transactions on Information Theory*, vol. 32, no. 1, pp. 85–96, Jan. 1986.
- [10] Ruxandra Lupas and Sergio Verdú, “Near-far resistance of multi-user detectors in asynchronous channels,” *IEEE Transactions on Communications*, vol. 38, no. 4, pp. 496–508, Apr. 1990.
- [11] Mahes K. Varanasi and Behnaam Aazhang, “Multistage detection in asynchronous code-division multiple-access communications,” *IEEE Transactions on Communications*, vol. 38, no. 4, pp. 509–519, Apr. 1990.

- [12] Zhenhua Xie, Robert T. Short, and Craig K. Rushforth, “A family of suboptimum detectors for coherent multiuser communications,” *IEEE Journal on Selected Areas in Communications*, vol. 8, no. 4, pp. 683–690, May 1990.
- [13] Shilpa Talwar, Mats Viberg, and Arogyaswami Paulraj, “Blind separation of synchronous co-channel digital signals using an antenna array—part I: Algorithms,” *IEEE Transactions on Signal Processing*, vol. 44, no. 5, pp. 1184–1197, May 1996.
- [14] Alle-Jan van der Veen, Shilpa Talwar, and Arogyaswami Paulraj, “Blind estimation of multiple digital signals transmitted over FIR channels,” *IEEE Signal Processing Letters*, vol. 2, no. 5, pp. 99–102, May 1995.
- [15] Claes Tidestav, Anders Ahlén, and Mikael Sternad, “Narrowband and broadband multiuser detection using a multivariable DFE,” in *Proceedings of PIMRC*, Toronto, Canada, Sept. 1995, vol. 2, pp. 732–736.
- [16] Claes Tidestav, “Optimum diversity combining in multi-user digital mobile telephone systems,” M.S. thesis, UPTEC 93094 E, Uppsala University, Uppsala, Sweden, Dec. 1993.
- [17] Alexandra Duel-Hallen, “Equalizers for multiple input/multiple output channels and PAM systems with cyclostationary input sequences,” *IEEE Journal on Selected Areas in Communications*, vol. 10, no. 3, pp. 630–639, Apr. 1992.
- [18] Lars Lindbom, *A Wiener Filtering Approach to the Design of Tracking Algorithms*, Ph.D. thesis, Uppsala University, Uppsala, Sweden, Nov. 1995.
- [19] Pierre A. Laurent, “Exact and approximate construction of digital phase modulations by superposition of amplitude modulated pulses (AMP),” *IEEE Transactions on Communications*, vol. 34, no. 2, pp. 150–160, Feb. 1986.
- [20] Jonas Karlsson, *Adaptive Antennas in GSM Systems with Non-Synchronized Base Stations*, Licentiate thesis, Royal Institute of Technology, Stockholm, Sweden, Mar. 1998.
- [21] David Asztély, “On antenna arrays in mobile communication systems, fast fading and GSM base station receiver algorithms,” M.S. thesis, Royal Institute of Technology, Stockholm, Sweden, Feb. 1995.
- [22] Sören Andersson, Mille Millnert, Mats Viberg, and Bo Wahlberg, “An adaptive array for mobile communication systems,” *IEEE Transactions on Vehicular Technology*, vol. 40, no. 1, pp. 230–236, Feb. 1991.
- [23] Tracy Fulghum, Karl Molnar, and Alexandra Duel-Hallen, “The Jakes fading model incorporating angular spread,” in *Proceedings of CISS*, Baltimore, USA, Mar. 1997.
- [24] Vladimír Kučera, *Analysis and Design of Discrete Linear Control Systems*, Prentice Hall, 1991.
- [25] John G. Proakis, *Digital Communications*, McGraw–Hill, New York, NY, second edition, 1989.

- [26] Mikael Sternad and Anders Ahlén, “The structure and design of realizable decision feedback equalizers for IIR channels with colored noise,” *IEEE Transactions on Information Theory*, vol. 36, no. 4, pp. 848–858, July 1990.
- [27] Sergio Verdú, “Optimum multiuser asymptotic efficiency,” *IEEE Transactions on Communications*, vol. 34, no. 9, pp. 890–897, Sept. 1986.
- [28] Claes Tidestav and Erik Lindskog, “Bootstrap equalization,” in *Proceedings of ICUPC*, Florence, Italy, Oct. 1998, to appear.
- [29] Sören Andersson, Ulf Forssén, Jonas Karlsson, Tom Witzschel, Peter Fischer, and Andreas Krug, “Ericsson/Mannesmann GSM field-trials with adaptive antennas,” in *Proceedings of the IEEE Vehicular Technology Conference*, Phoenix, USA, May 1997, vol. 3, pp. 1587–1591.
- [30] K. Giridhar, John J. Shynk, Amit Mathur, Sujai Chari, and Richard P. Gooch, “Non-linear techniques for the joint estimation of co-channel signals,” *IEEE Transactions on Communications*, vol. 45, no. 4, pp. 473–484, Apr. 1997.
- [31] Erik Lindskog, Anders Ahlén, and Mikael Sternad, “Spatio-temporal equalization for multipath environments in mobile radio applications,” in *Proceedings of the IEEE Vehicular Technology Conference*, Chicago, July 1995, vol. 1, pp. 399–403.
- [32] Lars Lindbom, *Adaptive Equalization for Fading Mobile Radio Channels*, Licentiate thesis, Uppsala University, Uppsala, Sweden, Nov. 1992.
- [33] Thomas Kailath, *Linear Systems*, Prentice Hall, 1980.

Appendix A

Remarks on the structure and design of the MIMO DFE

Apart from the filters having multiple inputs and multiple outputs, the FIR DFE (3.1) has the conventional structure of a decision feedback equalizer. A rarely noted fact is that, assuming correct past decisions, a DFE having an FIR structure can attain the minimal MSE *only* under the following assumptions:

1. The channel impulse response has finite length.
2. The additive noise is temporally white or autoregressive.

See [26] for a proof of this conclusion for the scalar case.

Assumption 1 is not restrictive for wireless channels. Assumption 2 however, is violated in a typical cellular system, since the main source of noise is co-channel interference, which has moving average, not autoregressive, statistics. In this paper, we will still consider the conventional (FIR) DFE structure. The main reason for this is that the error propagation resulting from incorrect past decisions would be more severe for an “optimal” DFE structure, since the impulse response of the feedback filter would have infinite length.

For the determination of the equalizer coefficients, we advocate an indirect approach. We thus suppose that an estimate of the channel impulse response (2.7) and the noise covariance function (2.4) has been made available to us. We then compute the *equalizer* matrix coefficients from the *channel* matrix coefficients and the noise covariance function. This is not the conventional approach in an adaptive setting, but the indirect approach has two major advantages in the present case:

1. The estimation of the channel parameters can be performed with better accuracy than direct estimation of the equalizer coefficients. When the channel has fewer inputs than outputs ($M < N$), fewer parameters have to be estimated based on the available data. For the indirect approach, only $M(L + 1)$ parameters describing the channels from the M users to a single antenna element have to be estimated simultaneously, based on data from that antenna and the training data for all users. In a direct approach, the feedforward filter of an equalizer which detects a single user must be tuned. If there are N antenna elements and the feedforward filter has $L + 1$ taps, the $N(L + 1)$ parameters describing this feedforward filter must be estimated simultaneously. See [31] for a performance comparison between indirectly and directly tuned MISO DFE:s.

2. The indirect approach is better suited for tracking of rapidly time-varying channels. This is due to the fact that channel parameters vary smoothly, whereas the corresponding optimum equalizer parameters do not. See [32] and [18] for a discussion.

Appendix B

Derivation of the MIMO MMSE DFE

Suppose that a linear time-invariant finite impulse response channel of order L is given by (2.6) and assume that

$$E[s(k)s^H(m)] = \delta_{km}I \quad E[v(k)v^H(m)] = \psi_{k-m} \quad E[s(k)v^H(m)] = 0. \quad (\text{B.1})$$

The objective is to estimate the symbol vector $s(k - \ell)$, by means of the *multiple-input-multiple-output decision feedback equalizer (MIMO DFE)* defined in (3.1), i.e.

$$\hat{s}(k - \ell|k) = \mathbf{S}(z^{-1})x(k) - \mathbf{Q}(z^{-1})\tilde{s}(k - \ell - 1) \quad (\text{B.2})$$

$$\begin{aligned} &= \mathbf{S}_0x(k) + \mathbf{S}_1x(k - 1) + \cdots + \mathbf{S}_{n_s}x(k - n_s) \\ &\quad - \mathbf{Q}_0\tilde{s}(k - \ell - 1) - \mathbf{Q}_1\tilde{s}(k - \ell - 2) - \cdots - \mathbf{Q}_{L+n_s-\ell-1}\tilde{s}(k - L - n_s) \end{aligned} \quad (\text{B.3})$$

$$\tilde{s}(k - \ell) = f(\hat{s}(k - \ell|k)) \quad (\text{B.4})$$

where $\mathbf{S}(z^{-1})$ of order n_s and $\mathbf{Q}(z^{-1})$ of order $n_Q = L + n_s - \ell - 1$ are polynomial matrices of dimension $N|M$ and $M|M$ respectively and $f(\cdot)$ is the decision non-linearity. Also,

$$\Theta_S^H = (\mathbf{S}_0 \quad \mathbf{S}_1 \quad \dots \quad \mathbf{S}_{n_s}) \quad (\text{B.5a})$$

$$\Theta_Q^H = (\mathbf{Q}_0 \quad \mathbf{Q}_1 \quad \dots \quad \mathbf{Q}_{L+n_s-\ell-1}) \quad (\text{B.5b})$$

and

$$\mathbf{x}_k = (x^T(k) \quad x^T(k - 1) \quad \dots \quad x^T(k - n_s))^T \quad (\text{B.6a})$$

$$\tilde{\mathbf{s}}_{k-\ell-1} = (\tilde{s}^T(k - \ell - 1) \quad \dots \quad \tilde{s}^T(k - n_s - L))^T. \quad (\text{B.6b})$$

The coefficients $\{\mathbf{S}_n\}$ and $\{\mathbf{Q}_n\}$ are to be determined so that the mean square error of the estimate $\hat{s}(k - \ell|k)$ is minimized under the constraint of *realizability*, which implies that the filters $\mathbf{S}(z^{-1})$ and $\mathbf{Q}(z^{-1})$ should be causal and the decision delay ℓ should be finite.

The estimation error

$$\varepsilon(k - \ell) = s(k - \ell) - \hat{s}(k - \ell|k) \quad (\text{B.7})$$

is minimized in the mean square sense if it is orthogonal to all signals which the estimate $\hat{s}(k - \ell|k)$ may be based upon, i.e. \mathbf{x}_k and $\tilde{\mathbf{s}}_{k-\ell-1}$. The matrix filter coefficients providing the minimum mean square estimation error are thus determined by the orthogonality

condition

$$E \left[\begin{pmatrix} \mathbf{x}_k \\ -\tilde{\mathbf{s}}_{k-\ell-1} \end{pmatrix} \varepsilon^H(k-\ell) \right] = 0 \quad (\text{B.8})$$

or, with $\varepsilon(k-\ell)$ from (B.7)

$$E \left[\begin{pmatrix} \mathbf{x}_k \\ -\tilde{\mathbf{s}}_{k-\ell-1} \end{pmatrix} \hat{s}^H(k-\ell|k) \right] = E \left[\begin{pmatrix} \mathbf{x}_k \\ -\tilde{\mathbf{s}}_{k-\ell-1} \end{pmatrix} s^H(k-\ell) \right].$$

Next, insert $\hat{s}(k-\ell|k)$ from (B.3):

$$\begin{pmatrix} E\mathbf{x}_k\mathbf{x}_k^H & -E\mathbf{x}_k\tilde{\mathbf{s}}_{k-\ell-1}^H \\ -E\tilde{\mathbf{s}}_{k-\ell-1}\mathbf{x}_k^H & E\tilde{\mathbf{s}}_{k-\ell-1}\tilde{\mathbf{s}}_{k-\ell-1}^H \end{pmatrix} \begin{pmatrix} \Theta_S \\ \Theta_Q \end{pmatrix} = \begin{pmatrix} E\mathbf{x}_k s^H(k-\ell) \\ -E\tilde{\mathbf{s}}_{k-\ell-1} s^H(k-\ell) \end{pmatrix}. \quad (\text{B.9})$$

Assume that all previous decisions were correct, i.e.

$$\tilde{s}(k-n) = s(k-n) \quad \forall \ell+1 \leq n \leq L+n_s$$

and define

$$\mathbf{s}_{k-\ell-1} = (s^T(k-\ell-1) \quad \dots \quad s^T(k-n_s-L))^T. \quad (\text{B.10})$$

Due to the assumption of uncorrelated symbols made in (B.1), equation (B.9) can then be simplified to

$$\begin{pmatrix} E\mathbf{x}_k\mathbf{x}_k^H & -E\mathbf{x}_k\mathbf{s}_{k-\ell-1}^H \\ -E\mathbf{s}_{k-\ell-1}\mathbf{x}_k^H & I \end{pmatrix} \begin{pmatrix} \Theta_S \\ \Theta_Q \end{pmatrix} = \begin{pmatrix} E\mathbf{x}_k s^H(k-\ell) \\ 0 \end{pmatrix}. \quad (\text{B.11})$$

To evaluate the expectations in (B.11), we invoke the channel model (2.6) to write $x(k-n)$ as

$$x(k-n) = (\mathbf{H}_0 \quad \dots \quad \mathbf{H}_L) \begin{pmatrix} s(k-n) \\ \vdots \\ s(k-n-L) \end{pmatrix} + v(k-n). \quad (\text{B.12})$$

By inserting (B.12) into (B.6a) for $0 \leq n \leq n_s$, we will obtain an explicit expression of \mathbf{x}_k in terms of the channel coefficient matrices:

$$\mathbf{x}_k = \begin{pmatrix} \mathbf{H}_0 & \dots & \mathbf{H}_L & \dots & 0 \\ \vdots & \ddots & & \ddots & \vdots \\ 0 & \dots & \mathbf{H}_0 & \dots & \mathbf{H}_L \end{pmatrix} \begin{pmatrix} s(k) \\ \vdots \\ s(k-n_s-L) \end{pmatrix} + \begin{pmatrix} v(k) \\ \vdots \\ v(k-n_s) \end{pmatrix}. \quad (\text{B.13})$$

To obtain a more compact expression of (B.13), we introduce the vector of stacked noise vectors

$$\mathbf{v}_k = (v^T(k) \quad v^T(k-1) \quad \dots \quad v^T(k-n_s))^T \quad (\text{B.14})$$

and the vector of stacked symbol vectors

$$\bar{\mathbf{s}}_k = (s^T(k) \quad s^T(k-1) \quad \dots \quad s^T(k-\ell+1))^T. \quad (\text{B.15})$$

Furthermore, we define the following matrices:

$$\begin{aligned} \mathcal{F}_{tot} &\triangleq \left\{ \begin{pmatrix} \mathbf{H}_0 & \dots & \mathbf{H}_L & 0 & \dots & 0 \\ 0 & \mathbf{H}_0 & \dots & \mathbf{H}_L & \ddots & \vdots \\ \vdots & \ddots & \ddots & \ddots & \ddots & 0 \\ 0 & \dots & \dots & \mathbf{H}_0 & \dots & \mathbf{H}_L \end{pmatrix} \right\} N(n_s + 1) \\ &\triangleq (\mathcal{F}_{fut} \quad \mathcal{F}_{pres} \quad \mathcal{F}_{past}) \end{aligned} \quad (\text{B.16a})$$

where we have defined

$$\mathcal{F}_{fut} \triangleq \text{The first } M\ell \text{ columns in } \mathcal{F}_{tot} \quad (\text{B.16b})$$

$$\mathcal{F}_{pres} \triangleq \text{Columns } M\ell + 1 \text{ to } M(\ell + 1) \text{ in } \mathcal{F}_{tot} \quad (\text{B.16c})$$

$$\mathcal{F}_{past} \triangleq \text{Columns } M(\ell + 1) + 1 \text{ to } M(n_s + L + 1) \text{ in } \mathcal{F}_{tot}. \quad (\text{B.16d})$$

Equation (B.13) can then be written as

$$\mathbf{x}_k = \mathcal{F}_{fut}\bar{\mathbf{s}}_k + \mathcal{F}_{pres}\mathbf{s}(k - \ell) + \mathcal{F}_{past}\mathbf{s}_{k-\ell-1} + \mathbf{v}_k \quad (\text{B.17})$$

where $\mathbf{s}_{k-\ell-1}$ was defined in (B.10). Using (B.17) and (B.1), we can compute the expectations in (B.11):

$$\begin{aligned} E[\mathbf{x}_k \mathbf{x}_k^H] &= \mathcal{F}_{fut} \mathcal{F}_{fut}^H + \mathcal{F}_{pres} \mathcal{F}_{pres}^H + \mathcal{F}_{past} \mathcal{F}_{past}^H + \Psi \\ E[\mathbf{x}_k \mathbf{s}_{k-\ell-1}^H] &= \mathcal{F}_{past} \\ E[\mathbf{x}_k \mathbf{s}^H(k - \ell)] &= \mathcal{F}_{pres} \end{aligned}$$

where Ψ is given by (3.8).

These computed expectations can then be inserted into the normal equations (B.11):

$$\begin{pmatrix} \mathcal{F}_{fut} \mathcal{F}_{fut}^H + \mathcal{F}_{pres} \mathcal{F}_{pres}^H + \mathcal{F}_{past} \mathcal{F}_{past}^H + \Psi & -\mathcal{F}_{past} \\ -\mathcal{F}_{past}^H & I \end{pmatrix} \begin{pmatrix} \Theta_S \\ \Theta_Q \end{pmatrix} = \begin{pmatrix} \mathcal{F}_{pres} \\ 0 \end{pmatrix}. \quad (\text{B.18})$$

By observing that $\Theta_Q = \mathcal{F}_{past}^H \Theta_S$ from the second block row of (B.18) and inserting this into the first block row, we obtain

$$(\mathcal{F}_{fut} \mathcal{F}_{fut}^H + \mathcal{F}_{pres} \mathcal{F}_{pres}^H + \Psi) \Theta_S = \mathcal{F}_{pres} \quad (\text{B.19a})$$

$$\Theta_Q = \mathcal{F}_{past}^H \Theta_S. \quad (\text{B.19b})$$

Now observe that $(\mathcal{F}_{fut} \quad \mathcal{F}_{pres}) = \mathcal{F}$ as defined in (3.7). Thus (B.19a) and (B.19b) can be expressed as

$$(\mathcal{F} \mathcal{F}^H + \Psi) \Theta_S = \mathcal{F}_{pres} \quad (\text{B.20a})$$

$$\Theta_Q = \mathcal{F}_{past}^H \Theta_S. \quad (\text{B.20b})$$

Here (B.20a) coincides with (3.6) and if we complex conjugate both sides of (B.20b) and evaluate for each matrix element \mathbf{Q}_n , we readily obtain (3.9). Equations (B.20a) and (B.20b) are the design equations for the multiple-input-multiple-output decision feedback equalizer.

Appendix C

Proof of Lemma 1

We will here prove that $M > N$ implies that $\mathbf{H}(z^{-1})$ and $z^{-\ell-1}\mathbf{I}_M$ have a common right divisor which is not a right divisor of $z^{-\ell}\mathbf{I}_M$. In this case, the ZF equation (3.4) will not have any solution.

If $\mathbf{H}(z^{-1})$ and $z^{-\ell-1}\mathbf{I}_M$ have a common right divisor $\mathbf{R}(z^{-1})$, we must have

$$\mathbf{H}(z^{-1}) = \tilde{\mathbf{H}}(z^{-1})\mathbf{R}(z^{-1}) \quad (\text{C.1a})$$

$$z^{-\ell-1}\mathbf{I}_M = \mathbf{A}(z^{-1})\mathbf{R}(z^{-1}) \quad (\text{C.1b})$$

for some polynomial matrices $\tilde{\mathbf{H}}(z^{-1})$, $\mathbf{R}(z^{-1})$ and $\mathbf{A}(z^{-1})$ of dimensions $N|M$, $M|M$ and $M|M$, respectively. We propose, that when $M > N$ such a common right divisor is given by

$$\mathbf{R}(z^{-1}) = \begin{pmatrix} \mathbf{I}_{M-1} & \mathbf{r}(z^{-1}) \\ 0 & z^{-\ell-1} \end{pmatrix} \quad (\text{C.2})$$

and that this polynomial matrix is not a right divisor of $z^{-\ell}\mathbf{I}_M$. In (C.2), $\mathbf{r}(z^{-1})$ is a polynomial column vector with $M - 1$ rows which will be specified later.

For $\mathbf{R}(z^{-1})$ in (C.2), we must thus verify the following three properties:

1. $\mathbf{R}(z^{-1})$ is a right divisor of $\mathbf{H}(z^{-1})$
2. $\mathbf{R}(z^{-1})$ is a right divisor of $z^{-\ell-1}\mathbf{I}_M$
3. $\mathbf{R}(z^{-1})$ is *not* a right divisor of $z^{-\ell}\mathbf{I}_M$.

Property 1

To show property 1, we partition $\mathbf{H}(z^{-1})$:

$$\mathbf{H}(z^{-1}) = (\mathbf{H}^{(1)}(z^{-1}) \quad \mathbf{H}^{(2)}(z^{-1})) , \quad (\text{C.3})$$

where $\mathbf{H}^{(1)}(z^{-1})$ constitutes the first $M - 1$ columns and $\mathbf{H}^{(2)}(z^{-1})$ the last column of $\mathbf{H}(z^{-1})$, respectively. In the same way, we also partition $\tilde{\mathbf{H}}(z^{-1})$, which was implicitly defined in (C.1a):

$$\tilde{\mathbf{H}}(z^{-1}) = (\tilde{\mathbf{H}}^{(1)}(z^{-1}) \quad \tilde{\mathbf{H}}^{(2)}(z^{-1})) . \quad (\text{C.4})$$

We now insert (C.3), (C.4) and (C.2) into (C.1a):

$$(\mathbf{H}^{(1)}(z^{-1}) \quad \mathbf{H}^{(2)}(z^{-1})) = (\tilde{\mathbf{H}}^{(1)}(z^{-1}) \quad \tilde{\mathbf{H}}^{(2)}(z^{-1})) \begin{pmatrix} \mathbf{I}_{M-1} & \mathbf{r}(z^{-1}) \\ 0 & z^{-\ell-1} \end{pmatrix}.$$

This equation is satisfied if

$$\mathbf{H}^{(1)}(z^{-1}) = \tilde{\mathbf{H}}^{(1)}(z^{-1}) \quad (C.5a)$$

$$\mathbf{H}^{(2)}(z^{-1}) = \tilde{\mathbf{H}}^{(1)}(z^{-1})\mathbf{r}(z^{-1}) + z^{-\ell-1}\tilde{\mathbf{H}}^{(2)}(z^{-1}). \quad (C.5b)$$

We can now insert (C.5a) into (C.5b):

$$\mathbf{H}^{(2)}(z^{-1}) = \mathbf{H}^{(1)}(z^{-1})\mathbf{r}(z^{-1}) + z^{-\ell-1}\mathbf{I}_N\tilde{\mathbf{H}}^{(2)}(z^{-1}). \quad (C.6)$$

This equation will have a solution $\{\mathbf{r}(z^{-1}), \tilde{\mathbf{H}}^{(2)}(z^{-1})\}$ if and only if every common *left* divisor of $\mathbf{H}^{(1)}(z^{-1})$ and $z^{-\ell-1}\mathbf{I}_N$ is also a left divisor of $\mathbf{H}^{(2)}(z^{-1})$. If this condition is satisfied, then a right divisor $\mathbf{R}(z^{-1})$ of the form (C.2) will exist. If it is not satisfied, then we exchange the single column $\mathbf{H}^{(2)}(z^{-1})$ for one of the columns in $\mathbf{H}^{(1)}(z^{-1})$. As we shall see, we can always use this trick to find a solution to equation (C.6).

To show this, assume the existence of a channel $\hat{\mathbf{H}}(z^{-1})$ such that no permutation of its columns will make (C.6) solvable. Define

$$\begin{aligned} \hat{\mathbf{H}}(z^{-1}) &\triangleq \left(\begin{array}{c|c} \hat{\mathbf{H}}^{(1)}(z^{-1}) & \hat{\mathbf{H}}^{(2)}(z^{-1}) \end{array} \right) \\ &\triangleq \left(\begin{array}{ccc|c} \hat{\mathbf{h}}_1(z^{-1}) & \dots & \hat{\mathbf{h}}_{M-1}(z^{-1}) & \hat{\mathbf{h}}_M(z^{-1}) \end{array} \right). \end{aligned}$$

Denote a set of M left divisors of $z^{-\ell-1}\mathbf{I}_N$ as $\{\mathbf{L}_m(z^{-1})\}_{m=1}^M$. If (C.6) lacks a solution for every permutation of the columns $\hat{\mathbf{h}}_i(z^{-1})$, $i = 1, \dots, M$, there must exist $M+1$ polynomial matrices $\Lambda_i(z^{-1})$, $i = 0, \dots, M$, such that

$$\begin{aligned} \Lambda_i(z^{-1}) &\text{ is a left divisor of } \hat{\mathbf{h}}_i(z^{-1}), \quad i = 1, \dots, M \\ \Lambda_0(z^{-1}) &\text{ is a left divisor of } z^{-\ell-1}\mathbf{I}_N. \end{aligned} \quad (C.7)$$

The polynomial matrices $\Lambda_i(z^{-1})$, $i = 0, \dots, M$ must have the following characterizing properties:

- (a) For $i \neq 0$, $\Lambda_i(z^{-1})$ must have all the polynomial matrices $\mathbf{L}_m(z^{-1})$, $m = 1, \dots, i-1, i+1, \dots, M$ as left divisors, i.e. we must be able to express $\Lambda_i(z^{-1})$ as

$$\Lambda_i(z^{-1}) = \mathbf{L}_m(z^{-1})\tilde{\Lambda}_i^m(z^{-1}), \quad \begin{matrix} i = 1, \dots, M \\ m = 1, \dots, i-1, i+1, \dots, M \end{matrix} \quad (C.8)$$

for some polynomial matrices $\tilde{\Lambda}_i^m(z^{-1})$.

- (b) $\Lambda_0(z^{-1})$ must have $\mathbf{L}_m(z^{-1})$, $m = 1, \dots, M$ as left divisors and, i.e. we must be able to write

$$\Lambda_0(z^{-1}) = \mathbf{L}_m(z^{-1})\tilde{\Lambda}_0^m(z^{-1}), \quad m = 1, \dots, M \quad (C.9)$$

for some polynomial matrices $\tilde{\Lambda}_0^m(z^{-1})$.

- (c) For any given $i \neq 0$, $\mathbf{L}_i(z^{-1})$ must *not* be a left divisor of $\Lambda_i(z^{-1})$. If $\mathbf{L}_i(z^{-1})$ were a left divisor of $\Lambda_i(z^{-1})$, the permutation $\hat{\mathbf{H}}^{(2)}(z^{-1}) = \hat{\mathbf{h}}_i(z^{-1})$ would imply that (C.6) has a solution: the polynomial matrix $\mathbf{L}_i(z^{-1})$ is the only left factor which is common to $\hat{\mathbf{H}}^{(1)}(z^{-1})$ and $z^{-\ell-1}\mathbf{I}_N$, and $\mathbf{L}_i(z^{-1})$ will be a left factor also to $\hat{\mathbf{H}}^{(2)}(z^{-1})$.
- (d) The set $\{\mathbf{L}_m(z^{-1})\}_{m=1}^M$ must have M elements, i.e. we must be able to find M left divisors $\mathbf{L}_i(z^{-1})$ of $z^{-\ell-1}\mathbf{I}_N$. Otherwise, there will be some permutation of the columns of $\hat{\mathbf{H}}(z^{-1})$ which makes it possible to find a solution to (C.6).

When the channel has left divisors as defined in (C.7), (C.8) and (C.9), $\hat{\mathbf{H}}^{(1)}(z^{-1})$ and $z^{-\ell-1}\mathbf{I}_N$ will have a common left divisor $\mathbf{L}_M(z^{-1})$ which is not a left divisor of $\hat{\mathbf{H}}^{(2)}(z^{-1}) = \hat{\mathbf{h}}_M(z^{-1})$, no matter how we arrange the columns of $\hat{\mathbf{H}}(z^{-1})$. However, if we cannot find such a set of polynomial matrices $\mathbf{L}_i(z^{-1})$, then some permutation of the columns of $\hat{\mathbf{H}}(z^{-1})$ will make it possible to solve (C.6). We will now show that it is indeed impossible to find a set $\{\mathbf{L}_i(z^{-1})\}_{i=1}^M$ such that (a), (b), (c) and (d) are all satisfied.

Without restriction, we assume that both $\Lambda_i(z^{-1})$ and $\mathbf{L}_i(z^{-1})$ are written in *Hermite form*. A Hermite form polynomial matrix is upper triangular and row reduced. Furthermore, the element with the highest degree in each row is the diagonal element.

To see under what conditions (c) is satisfied, we study the left *matrix fraction descriptions (MFD:s)*

$$\mathbf{D}_i(z^{-1}) \stackrel{\Delta}{=} \Lambda_i^{-1}(z^{-1}) \mathbf{L}_i(z^{-1}) \quad i = 1, \dots, M \quad (\text{C.10})$$

which can be rewritten

$$\Lambda_i(z^{-1}) = \mathbf{L}_i(z^{-1}) \mathbf{D}_i^{-1}(z^{-1}). \quad (\text{C.11})$$

In general, $\mathbf{D}_i^{-1}(z^{-1})$ is a rational matrix. However, if $\mathbf{D}_i^{-1}(z^{-1})$ can be shown to be a polynomial matrix in z^{-1} , then $\mathbf{L}_i(z^{-1})$ will be a left divisor of $\Lambda_i(z^{-1})$. To satisfy (c), we must thus assure that $\mathbf{D}_i^{-1}(z^{-1})$ is not a polynomial matrix in z^{-1} .

In fact, it turns out that as soon as $\mathbf{D}_i(z^{-1})$ is a proper rational matrix¹, $\mathbf{D}_i^{-1}(z^{-1})$ will be a polynomial matrix. To see this, we observe that since $\Lambda_0(z^{-1})$ is a left factor of $z^{-\ell-1}\mathbf{I}_N$,

$$\begin{aligned} \det z^{-\ell-1}\mathbf{I}_N &= \det(\Lambda_0(z^{-1})\Psi(z^{-1})) = \det \Lambda_0(z^{-1}) \det \Psi(z^{-1}) \\ &= \det \mathbf{L}_i(z^{-1}) \det \tilde{\Lambda}_0^i(z^{-1}) \det \Psi(z^{-1}) \end{aligned}$$

for any i and some polynomial matrix $\Psi(z^{-1})$. But, since

$$\det z^{-\ell-1}\mathbf{I}_N = z^{-N(\ell+1)}$$

we must have

$$\det \mathbf{L}_i(z^{-1}) = z^{-\alpha_i}$$

for some non-negative number α_i . Using this, we obtain from (C.10)

$$\det \mathbf{D}_i(z^{-1}) = \frac{\det \mathbf{L}_i(z^{-1})}{\det \Lambda_i(z^{-1})} = \frac{1}{z^{-\Gamma_i}}$$

¹For each scalar element in a proper rational matrix, the degree (in z^{-1}) of the numerator polynomial is smaller than or equal to the degree (in z^{-1}) of the corresponding denominator polynomial.

for some constant Γ_i . Also,

$$\mathbf{D}_i^{-1}(z^{-1}) = \frac{\text{Adj } \mathbf{D}_i(z^{-1})}{\det \mathbf{D}_i(z^{-1})} = z^{-\Gamma_i} \text{Adj } \mathbf{D}_i(z^{-1}).$$

Now, assume that $\mathbf{D}_i(z^{-1})$ is proper. This means that $\Gamma_i \geq 0$. Each element in $\text{Adj } \mathbf{D}_i(z^{-1})$ is a minor of $\mathbf{D}_i(z^{-1})$. Since $\mathbf{D}_i(z^{-1})$ is row-reduced, the degree of every minor is less than or equal to the degree of the determinant. Therefore, $\mathbf{D}_i^{-1}(z^{-1})$ becomes a polynomial matrix in z^{-1} . Thus, if the MFD (C.10) is proper, we see from (C.11) that condition (c) is violated. If we can find only one index i for which $\mathbf{D}_i(z^{-1})$ in the MFD (C.10) is proper, equation (C.6) can be solved with the permutation $\hat{\mathbf{H}}_2(z^{-1}) = \hat{\mathbf{h}}_i(z^{-1})$. Thus, condition (c) can be satisfied only if the rational matrix $\mathbf{D}_i(z^{-1})$, defined in (C.10), is improper for all $i = 1, \dots, M$.

To find the conditions under which the rational matrix $\mathbf{D}_i(z^{-1})$ is improper, we define

$$\begin{aligned}\mathbf{L}_i^r(z^{-1}) &\stackrel{\Delta}{=} \text{row } r \text{ in } \mathbf{L}_i(z^{-1}) \\ \mathbf{\Lambda}_i^r(z^{-1}) &\stackrel{\Delta}{=} \text{row } r \text{ in } \mathbf{\Lambda}_i(z^{-1}).\end{aligned}$$

Since both $\mathbf{\Lambda}_i(z^{-1})$ and $\mathbf{L}_i(z^{-1})$ are row reduced, the left MFD $\mathbf{D}_i(z^{-1})$ is improper if and only if [33]

$$\deg \mathbf{L}_i^r(z^{-1}) > \deg \mathbf{\Lambda}_i^r(z^{-1}) \quad (\text{C.12})$$

for some row r .

Let us now study $\deg \mathbf{\Lambda}_i^r(z^{-1})$. Assume that of all the left divisors $\mathbf{L}_m(z^{-1})$ in $\mathbf{\Lambda}_i(z^{-1})$, $\mathbf{L}_\nu(z^{-1})$ has the highest degree in row r , i.e.

$$\deg \mathbf{L}_\nu^r(z^{-1}) = \max_{m \neq i} \deg (\mathbf{L}_m^r(z^{-1})) . \quad (\text{C.13})$$

We now write $\mathbf{\Lambda}_i^r(z^{-1})$ as

$$\mathbf{\Lambda}_i^r(z^{-1}) = \mathbf{L}_\nu^r(z^{-1}) \tilde{\mathbf{\Lambda}}_i^\nu(z^{-1})$$

and define the following scalar polynomials:

$$\begin{aligned}\lambda_{rr}(z^{-1}) &\stackrel{\Delta}{=} \text{element } r \text{ in the polynomial vector } \mathbf{\Lambda}_i^r(z^{-1}) \\ L_{rr}(z^{-1}) &\stackrel{\Delta}{=} \text{element } r \text{ in the polynomial vector } \mathbf{L}_\nu^r(z^{-1}) \\ \tilde{\lambda}_{rr}(z^{-1}) &\stackrel{\Delta}{=} \text{element } r, r \text{ in the polynomial matrix } \tilde{\mathbf{\Lambda}}_i^\nu(z^{-1}).\end{aligned}$$

Due to the Hermite form assumption made on $\mathbf{\Lambda}_i(z^{-1})$, the degree of $\mathbf{\Lambda}_i^r(z^{-1})$ is determined by the degree of $\lambda_{rr}(z^{-1})$. Also, when $\mathbf{\Lambda}_i(z^{-1})$ and $\mathbf{L}_i(z^{-1})$ are upper triangular, so is $\tilde{\mathbf{\Lambda}}_i(z^{-1})$. When $\mathbf{L}_i(z^{-1})$ and $\tilde{\mathbf{\Lambda}}_i(z^{-1})$ are both triangular,

$$\lambda_{rr}(z^{-1}) = L_{rr}(z^{-1}) \tilde{\lambda}_{rr}(z^{-1}) .$$

Therefore,

$$\begin{aligned}\deg \mathbf{\Lambda}_i^r(z^{-1}) &= \deg \lambda_{rr}(z^{-1}) = \deg (L_{rr}(z^{-1}) \tilde{\lambda}_{rr}(z^{-1})) \\ &\geq \deg L_{rr}(z^{-1}) = \deg \mathbf{L}_\nu^r(z^{-1}) .\end{aligned} \quad (\text{C.14})$$

If we combine (C.12), (C.13) and (C.14), we see that a necessary condition for the existence of an improper $\mathbf{D}_i(z^{-1})$ is that there exists a row r in $\mathbf{L}_i(z^{-1})$ such that

$$\deg \mathbf{L}_i^r(z^{-1}) > \max_{m \neq i} \deg \mathbf{L}_m^r(z^{-1}). \quad (\text{C.15})$$

To make *every* $\mathbf{D}_i(z^{-1})$ improper, the inequality (C.15) must hold for every $i = 1, \dots, M$. This means that every $\mathbf{L}_i(z^{-1})$ must have a row, whose degree is greater than the degree of the corresponding row in all the other left factors $\mathbf{L}_m(z^{-1})$, $m \neq i$. Since for each of the N rows, only one of the M left factors $\mathbf{L}_i(z^{-1})$ can have the highest degree, we conclude there can be at most one left factor with the required property (C.15) for each particular row r . Therefore, when (c) is fulfilled we can find at most N such divisors, and when $M > N$ there will be no set of M left divisors as required by (d). Consequently, (C.6) will always have a solution and we can always find a polynomial matrix $\mathbf{R}(z^{-1})$ of the form (C.2) which is a right divisor to $\mathbf{H}(z^{-1})$.

Property 2

We immediately see that $\mathbf{R}(z^{-1})$ in (C.2) is a right divisor of $z^{-\ell-1}\mathbf{I}_M$, since

$$\begin{pmatrix} z^{-\ell-1}\mathbf{I}_{M-1} & -\mathbf{r}(z^{-1}) \\ 0 & 1 \end{pmatrix} \begin{pmatrix} \mathbf{I}_{M-1} & \mathbf{r}(z^{-1}) \\ 0 & z^{-\ell-1} \end{pmatrix} = z^{-\ell-1}\mathbf{I}_M.$$

Property 3

To prove that $\mathbf{R}(z^{-1})$ is not a right divisor of $z^{-\ell}\mathbf{I}_M$, we will try to find a polynomial matrix $\mathbf{B}(z^{-1})$ such that

$$z^{-\ell}\mathbf{I}_M = \mathbf{B}(z^{-1})\mathbf{R}(z^{-1}). \quad (\text{C.16})$$

We now partition $\mathbf{B}(z^{-1})$ into four blocks:

$$\mathbf{B}(z^{-1}) = \begin{pmatrix} \mathbf{B}_{11}(z^{-1}) & \mathbf{B}_{12}(z^{-1}) \\ \mathbf{B}_{21}(z^{-1}) & B_{22}(z^{-1}) \end{pmatrix},$$

where $\mathbf{B}_{11}(z^{-1})$ is $M-1|M-1$, $\mathbf{B}_{12}(z^{-1})$ is $M-1|1$, $\mathbf{B}_{21}(z^{-1})$ is $1|M-1$ and $B_{22}(z^{-1})$ is a scalar polynomial.

Equation (C.16) can now be expressed as

$$\begin{pmatrix} z^{-\ell}\mathbf{I}_{M-1} & 0 \\ 0 & z^{-\ell} \end{pmatrix} = \begin{pmatrix} \mathbf{B}_{11}(z^{-1}) & \mathbf{B}_{12}(z^{-1}) \\ \mathbf{B}_{21}(z^{-1}) & B_{22}(z^{-1}) \end{pmatrix} \begin{pmatrix} \mathbf{I}_{M-1} & \mathbf{r}(z^{-1}) \\ 0 & z^{-\ell-1} \end{pmatrix}. \quad (\text{C.17})$$

To fulfill (C.17), the following relations must hold:

$$z^{-\ell}\mathbf{I}_{M-1} = \mathbf{B}_{11}(z^{-1}) \quad (\text{C.18a})$$

$$0 = \mathbf{B}_{11}(z^{-1})\mathbf{r}(z^{-1}) + z^{-\ell-1}\mathbf{B}_{12}(z^{-1}) \quad (\text{C.18b})$$

$$0 = \mathbf{B}_{21}(z^{-1}) \quad (\text{C.18c})$$

$$z^{-\ell} = \mathbf{B}_{21}(z^{-1})\mathbf{r}(z^{-1}) + z^{-\ell-1}B_{22}(z^{-1}), \quad (\text{C.18d})$$

or equivalently

$$\mathbf{B}_{11}(z^{-1}) = z^{-\ell} \mathbf{I}_{M-1} \quad (\text{C.19a})$$

$$\mathbf{B}_{12}(z^{-1}) = -z \mathbf{r}(z^{-1}) \quad (\text{C.19b})$$

$$\mathbf{B}_{21}(z^{-1}) = 0 \quad (\text{C.19c})$$

$$B_{22}(z^{-1}) = z. \quad (\text{C.19d})$$

However, $\mathbf{B}(z^{-1})$ is required to be a polynomial matrix in z^{-1} , which is obviously violated by (C.19d). Therefore we conclude that $\mathbf{R}(z^{-1})$ cannot be a right divisor of $z^{-\ell} \mathbf{I}_M$.

Since all three claimed properties of $\mathbf{R}(z^{-1})$ have been established, the zero-forcing equation (3.4) cannot have a solution if $M > N$.

Appendix D

Proof of Theorem 2

We shall here derive the degree conditions (3.15), (3.16) and (3.17). If these conditions are fulfilled as well as (3.10), a *multiple-input-multiple-output zero-forcing decision feedback equalizer (MIMO ZF DFE)* will exist.

We start by verifying the condition (3.17). Equation (3.4) can be rewritten as

$$\mathbf{S}(z^{-1})\mathbf{H}(z^{-1}) = z^{-\ell}(\mathbf{I}_M + z^{-1}\mathbf{Q}(z^{-1})) . \quad (\text{D.1})$$

The polynomial matrix $\mathbf{Q}(z^{-1})$ must be chosen so that the degree of the right hand side equals the degree of the left hand side. The degree of the right hand side equals

$$\deg z^{-\ell}(\mathbf{I}_M + z^{-1}\mathbf{Q}(z^{-1})) = \deg z^{-\ell} + \deg(\mathbf{I}_M + z^{-1}\mathbf{Q}(z^{-1})) = \ell + n_Q + 1 .$$

whereas for the left hand side

$$\deg \mathbf{S}(z^{-1})\mathbf{H}(z^{-1}) \leq \deg \mathbf{S}(z^{-1}) + \deg \mathbf{H}(z^{-1}) = n_s + L .$$

For a given feedforward filter $\mathbf{S}(z^{-1})$ of degree n_s , a the feedback filter degree

$$n_Q \geq L + n_s - \ell - 1 \quad (\text{D.2})$$

is then sufficient to cancel all postcursor taps. The inequality (D.2) coincides with (3.17).

To prove the degree conditions (3.15) and (3.16), we first need to remove the influence of common factors within each column of $\mathbf{H}(z^{-1})$. For this purpose, we insert the factorization (3.11) into (D.1):

$$\mathbf{S}(z^{-1})\bar{\mathbf{H}}(z^{-1})\mathbf{G}(z^{-1})\mathbf{D}(z^{-1}) = z^{-\ell}(\mathbf{I}_M + z^{-1}\mathbf{Q}(z^{-1})) .$$

For this equation to have a solution, we must choose $\mathbf{Q}(z^{-1})$ so that the right divisor $\mathbf{G}(z^{-1})\mathbf{D}(z^{-1})$ of the left hand side is also a right divisor of the right hand side, i.e. we must have

$$z^{-\ell}(\mathbf{I}_M + z^{-1}\mathbf{Q}(z^{-1})) = \mathbf{X}(z^{-1})\mathbf{G}(z^{-1})\mathbf{D}(z^{-1}) \quad (\text{D.3})$$

for some matrix polynomial $\mathbf{X}(z^{-1})$. We realize that $\mathbf{D}(z^{-1})$ cannot be a right divisor of $\mathbf{I}_M + z^{-1}\mathbf{Q}(z^{-1})$, since the coefficients having the lowest degree differ when the propagation delay d_j is non-zero for some column j . However, the left hand side of (D.3) can be rewritten as

$$z^{-\ell}(\mathbf{I}_M + z^{-1}\mathbf{Q}(z^{-1})) = (\mathbf{I}_M + z^{-1}\mathbf{Q}(z^{-1}))z^{-\ell}\mathbf{I}_M$$

which has $\mathbf{D}(z^{-1})$ as a right divisor, since $d_j \leq \ell$ for all j by (3.13a). Therefore, we can write

$$\begin{aligned} z^{-\ell}(\mathbf{I}_M + z^{-1}\mathbf{Q}(z^{-1})) &= (\mathbf{I}_M + z^{-1}\mathbf{Q}(z^{-1}))z^{-\ell}\mathbf{I}_M \\ &= \mathbf{Y}(z^{-1})\bar{\mathbf{D}}(z^{-1})\mathbf{D}(z^{-1}) \end{aligned} \quad (\text{D.4})$$

for some matrix polynomial $\mathbf{Y}(z^{-1})$ and with

$$\bar{\mathbf{D}}(z^{-1}) = \text{diag}(z^{-\ell+d_1} \ \dots \ z^{-\ell+d_M}).$$

We now choose $\mathbf{Y}(z^{-1})$ so that it has $\mathbf{G}(z^{-1})$ as a right divisor, or equivalently

$$z^{-\ell}(\mathbf{I}_M + z^{-1}\mathbf{Q}(z^{-1})) = \bar{\mathbf{Y}}(z^{-1})\mathbf{G}(z^{-1})\bar{\mathbf{D}}(z^{-1})\mathbf{D}(z^{-1}). \quad (\text{D.5})$$

The matrix coefficient with the lowest degree on the left hand of (D.5) side must be equal to the matrix coefficient with the lowest degree on the right hand side. Since $\mathbf{G}(z^{-1})$ is monic, this can only be satisfied if $\bar{\mathbf{Y}}(z^{-1})$ is also monic, i.e. if

$$\bar{\mathbf{Y}}(z^{-1}) = \mathbf{I}_M + z^{-1}\bar{\mathbf{Q}}(z^{-1})$$

for some polynomial matrix $\bar{\mathbf{Q}}(z^{-1})$. If we insert $\bar{\mathbf{Y}}(z^{-1})$ into (D.5), we obtain

$$z^{-\ell}(\mathbf{I}_M + z^{-1}\mathbf{Q}(z^{-1})) = (\mathbf{I}_M + z^{-1}\bar{\mathbf{Q}}(z^{-1}))\mathbf{G}(z^{-1})\bar{\mathbf{D}}(z^{-1})\mathbf{D}(z^{-1}).$$

Since $\mathbf{G}(z^{-1})$ and $\bar{\mathbf{D}}(z^{-1})$ are diagonal, they commute. Hence

$$z^{-\ell}(\mathbf{I}_M + z^{-1}\mathbf{Q}(z^{-1})) = (\mathbf{I}_M + z^{-1}\bar{\mathbf{Q}}(z^{-1}))\bar{\mathbf{D}}(z^{-1})\mathbf{G}(z^{-1})\mathbf{D}(z^{-1}). \quad (\text{D.6})$$

From (D.6) we see that $z^{-\ell}(\mathbf{I}_M + z^{-1}\mathbf{Q}(z^{-1}))$ has $\mathbf{G}(z^{-1})\mathbf{D}(z^{-1})$ as a right factor as required. This factor can thus be removed in our original equation (D.1). We must now solve

$$\mathbf{S}(z^{-1})\bar{\mathbf{H}}(z^{-1}) = (\mathbf{I}_M + z^{-1}\bar{\mathbf{Q}}(z^{-1}))\bar{\mathbf{D}}(z^{-1}). \quad (\text{D.7})$$

with respect to $\mathbf{S}(z^{-1})$ and $\bar{\mathbf{Q}}(z^{-1})$. The polynomial matrix $\mathbf{Q}(z^{-1})$ which solves the original Diophantine equation (D.1) can then be obtained from the solution of (D.6).

Let us now investigate the equalized channel from sources 1 to M to the estimate of source j , i.e. let us consider row j in (D.7):

$$\sum_{k=1}^N \bar{H}_{km}(z^{-1})S_{jk}(z^{-1}) = z^{-\ell+d_m-1}\bar{Q}_{jm}(z^{-1}) \quad m \neq j \quad (\text{D.8a})$$

$$\sum_{k=1}^N \bar{H}_{kj}(z^{-1})S_{jk}(z^{-1}) = z^{-\ell+d_j}(1 + z^{-1}\bar{Q}_{jj}(z^{-1})). \quad (\text{D.8b})$$

Since we know there exist both ZF MIMO DFE:s and ZF MISO DFE:s when (3.10) holds, equations (D.8a) and (D.8b) can be solved if there are more unknowns than there are equations. In general, they can *not* be solved if the number of equations exceeds the number of unknowns.

The MIMO DFE

In the MIMO DFE, we must use the feedforward filter to cancel the precursor taps, and also to make the reference tap equal to the identity matrix. In the $M - 1$ equations in (D.8a), there are

$$\sum_{m \neq j} (\ell + 1 - d_m) \quad (D.9)$$

precursor taps which must be canceled. In (D.8b), the $\ell - d_j$ precursor taps must be canceled and the reference tap should be set to unity, giving

$$\ell + 1 - d_j \quad (D.10)$$

additional linear equations. Adding (D.9) and (D.10) gives the total number of conditions to fulfill:

$$\sum_{m=1}^M (\ell + 1 - d_m) = M(\ell + 1) - \sum_{m=1}^M d_m. \quad (D.11)$$

To satisfy these equations we must use only the feedforward filter. The feedforward filter for user j has $n_s + 1$ vector taps, giving a total of

$$N(n_s + 1) \quad (D.12)$$

unknowns. If we compare (D.11) with (D.12), we see that if

$$n_s \geq \frac{M(\ell + 1) - \sum_{m=1}^M d_m}{N} - 1 \quad (D.13)$$

all precursor taps can be canceled. Since (D.13) is independent of j , a feedforward filter degree satisfying (D.13) is generically necessary to fulfill the zero-forcing condition (3.3) for all M users. Together with (D.2), the condition (D.13) is sufficient for the existence of a zero-forcing MIMO DFE.

The MISO DFE

For the MISO DFE, we can only use the feedback filter to cancel the postcursor taps of the user we are detecting. The postcursor taps from the interfering users have to be canceled by the feedforward filter. Using only the feedforward filter, we must thus satisfy

$$\sum_{k=1}^N \bar{H}_{km}(z^{-1}) S_{jk}(z^{-1}) \equiv 0 \quad m \neq j \quad (D.14a)$$

$$\sum_{k=1}^N \bar{H}_{kj}(z^{-1}) S_{jk}(z^{-1}) = z^{-\ell+d_j} (1 + z^{-1} \bar{Q}_{jj}(z^{-1})). \quad (D.14b)$$

The $M - 1$ equations in (D.14a) now contribute one equation for each tap in the equalized channel giving

$$\sum_{m \neq j} (n_s + \bar{L}_m + 1) \quad (D.15)$$

linear equations, whereas the number of equations in (D.14b) is still equal to

$$\ell + 1 - d_j . \quad (\text{D.16})$$

This means that for user j we now have to satisfy

$$\sum_{m \neq j} (n_s + \bar{L}_m + 1) + \ell + 1 - d_j = (M - 1)(n_s + 1) + \sum_{m=1}^M (\bar{L}_m) - \bar{L}_j + \ell + 1 - d_j \quad (\text{D.17})$$

linear equations, whereas the number of unknowns is still given by (D.12). Thus, we require

$$n_s \geq \frac{\sum_{m=1}^M (\bar{L}_m) + \ell + 1 - \bar{L}_j - d_j}{N - M + 1} - 1 \quad (\text{D.18})$$

for each user. A feedforward filter degree

$$n_s \geq \max_j \frac{\sum_{m=1}^M (\bar{L}_m) + \ell + 1 - \bar{L}_j - d_j}{N - M + 1} - 1 \quad (\text{D.19})$$

is then generically necessary to fulfill the zero-forcing condition (3.3) for all M users. The conditions (D.2) and (D.19) are together sufficient to ensure the existence of a zero-forcing MISO DFE.